

Stilbene–Chalcone Hybrids: Design, Synthesis, and Evaluation as a New Class of Antimalarial Scaffolds That Trigger Cell Death through Stage Specific Apoptosis

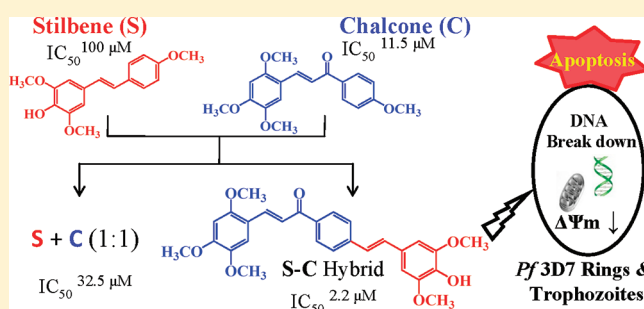
Naina Sharma,^{†,||} Dinesh Mohanakrishnan,^{‡,||} Amit Shard,[†] Abhishek Sharma,^{†,§} Saima,[†] Arun K. Sinha,^{*,†} and Dinkar Sahal^{*,‡}

[†]Natural Plant Products Division, CSIR-Institute of Himalayan Bioresource Technology, Palampur (H.P.) 176061, India

[‡]Malaria Research Laboratory, International Centre for Genetic Engineering and Biotechnology, Aruna Asaf Ali Marg, New Delhi 110067, India

Supporting Information

ABSTRACT: Novel stilbene–chalcone (S-C) hybrids were synthesized via a sequential Claisen–Schmidt–Knoevenagel–Heck approach and evaluated for antiplasmodial activity in *in vitro* red cell culture using SYBR Green I assay. The most potent hybrid (**11**) showed IC_{50} of 2.2, 1.4, and 6.4 μ M against 3D7 (chloroquine sensitive), Indo, and Dd2 (chloroquine resistant) strains of *Plasmodium falciparum*, respectively. Interestingly, the respective individual stilbene ($IC_{50} > 100 \mu$ M), chalcone ($IC_{50} = 11.5 \mu$ M), or an equimolar mixture of stilbene and chalcone ($IC_{50} = 32.5 \mu$ M) were less potent than **11**. Studies done using specific stage enriched cultures and parasite in continuous culture indicate that **11** and **18** spare the schizont but block the progression of the parasite life cycle at the ring or the trophozoite stages. Further, **11** and **18** caused chromatin condensation, DNA fragmentation, and loss of mitochondrial membrane potential in *Plasmodium falciparum*, thereby suggesting their ability to cause apoptosis in malaria parasite.



INTRODUCTION

Malaria, one of the most devastating infectious diseases, affects almost half of the global population and poses a major socioeconomic hazard to humanity at large.¹ The above grim scenario is further aggravated by the persistent tendency of *Plasmodium falciparum*, the most common malarial parasite, to rapidly develop resistance against any newly introduced drug.² In fact some recent reports have already indicated tolerance of this parasite toward artemisinin and its derivatives,³ the current World Health Organization prescribed gold standards against chloroquine (CQ) resistant malaria.⁴

Recently the concept of hybrid antimalarials⁵ has attracted much attention for tackling the alarming problem of drug resistance, as these molecules often act on multiple therapeutic targets because of the presence of two different, covalently fused pharmacophores.⁶ Some hybrid molecules (Figure 1),

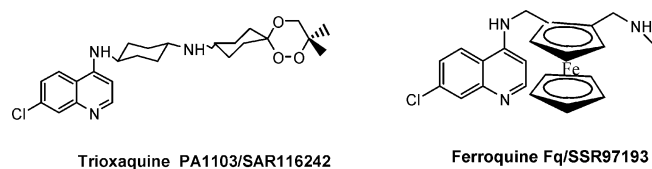


Figure 1. Some representative hybrid antimalarial drugs.

e.g., trioxaquine^{7a} and ferroquine^{7b} comprising 1,2,4-trioxane (4-aminoquinoline) and ferrocene–chloroquine moieties, respectively, are under clinical trials as hybrid antimalarial agents. In order to further reduce the probability of cross-resistance,⁸ there is also an urgent need to explore conceptually newer hybrid scaffolds, as the various prevalent hybrid antimalarials are structurally analogous to existing drugs.^{2b}

In this context, hydroxy substituted stilbenes and chalcones, two important classes of plant secondary metabolites, are promising candidates, as these individually possess multifarious pharmacological profiles⁹ including antimalarial activities.¹⁰ Even as stilbenes and chalcones share overlapping biosynthetic pathways, it seems that nature never attempted to form a hybrid of the two. To the best of our knowledge, the hybridization of these two pharmacophores into novel scaffolds and evaluation of their biological activities have not yet been reported. Herein, we describe a one-pot approach for the synthesis of such hydroxystilbene–chalcone hybrids and evaluation of their antimalarial activity against both CQ sensitive and resistant strains of *Plasmodium falciparum*.

Received: September 13, 2011

Published: November 18, 2011

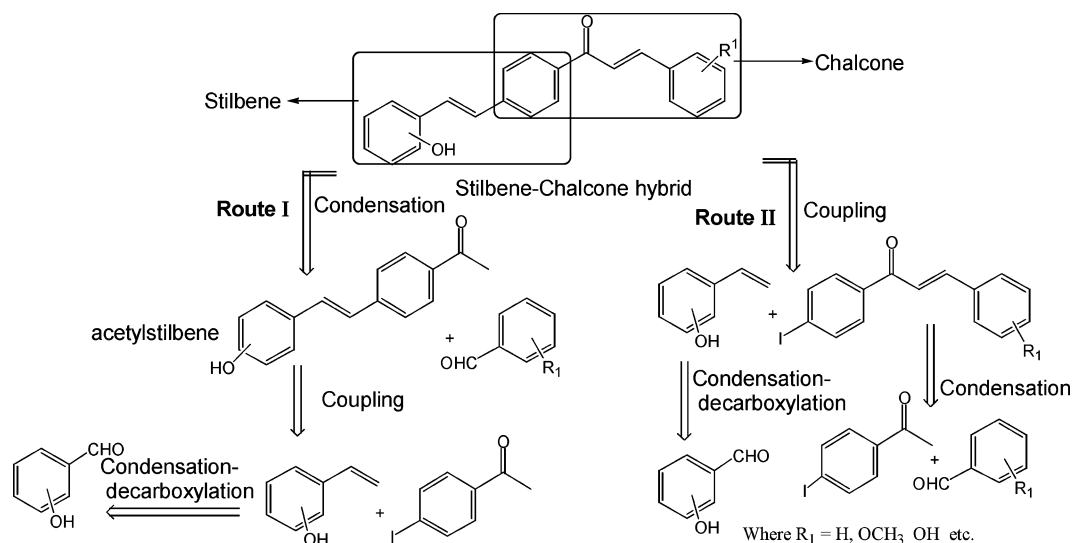
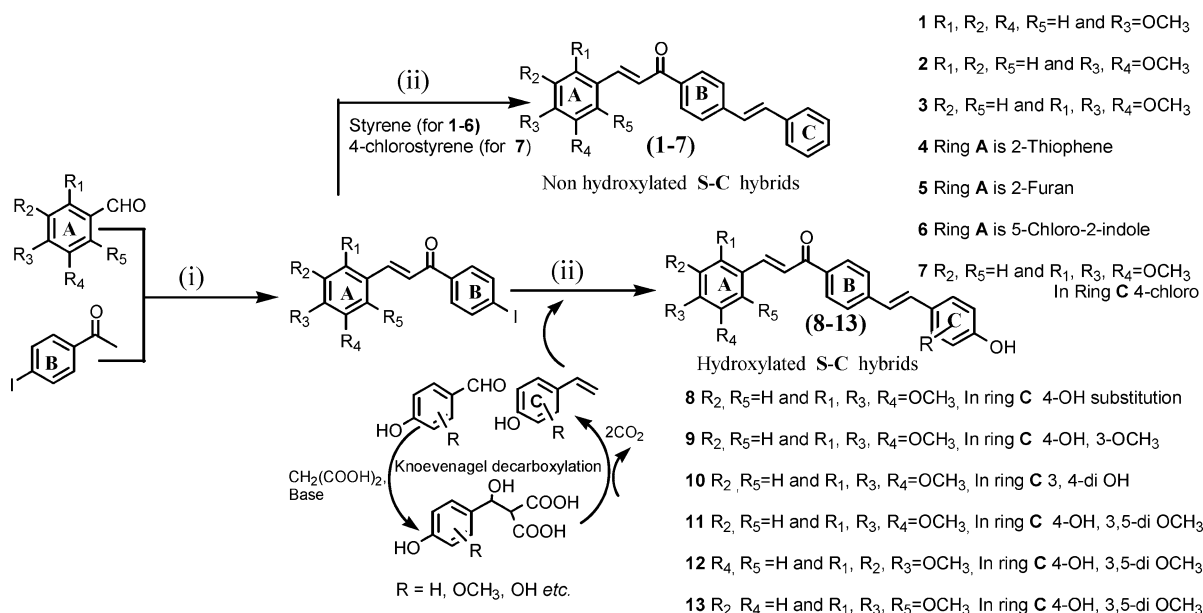


Figure 2. Retrosynthetic approaches for stilbene–chalcone hybrids.

Scheme 1^a



^aReagents and conditions: (i) NaOH, MeOH at room temp, 8 h; (ii) Pd(PPh₃)₄, DMF, piperidine, LiCl, reflux, 14 h.

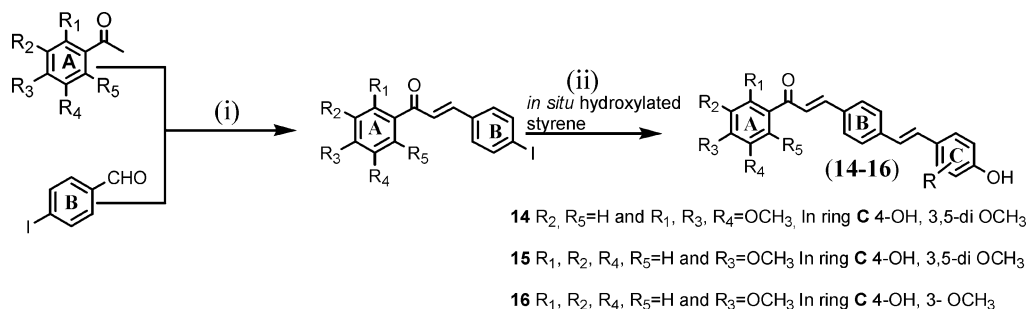
RESULTS AND DISCUSSION

Chemistry. In order to realize a facile access toward stilbene–chalcone hybrids from readily available substrates, two contrasting retrosynthetic approaches were visualized (Figure 2). Route I involved a Knoevenagel condensation–decarboxylation sequence¹¹ to afford hydroxylated styrene which can be further coupled with bromoacetophenone/iodoacetophenone via Heck coupling, leading to the formation of 4-acetylstilbene. Subsequently, the above 4-acetylstilbene can undergo Claisen–Schmidt condensation with substituted benzaldehydes to give the respective S-C hybrid. In the second approach, a Claisen–Schmidt condensation reaction provides bromo/iodo substituted chalcone which is subjected to Heck coupling.

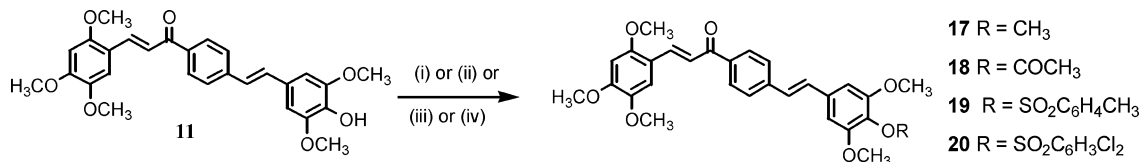
After a comparative evaluation of the above two strategies, route I involving an initial Knoevenagel–Doebner condensation step was not deemed to be favorable, as the presence of both *p*-iodoacetophenone and excess hydroxy substituted

benzaldehyde in the reaction mixture (Figure 2) could lead to the formation of the respective hydroxychalcone as side product, besides the formation of the expected acetylstilbene. Moreover, the subsequent step, i.e., Claisen–Schmidt condensation, could also lead to lower reaction performance due to the presence of hydroxy substitution on acetylstilbene (Figure 2). On the other hand, the above concerns were clearly circumvented in the second approach (route II, Figure 2), and thus, it was adopted for the synthesis of various stilbene–chalcone hybrids.

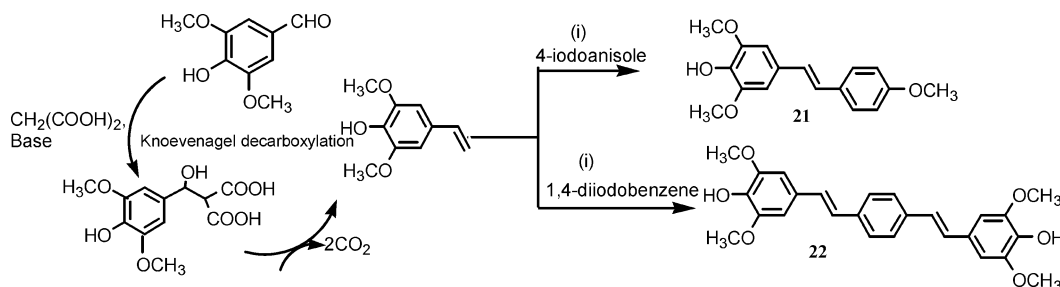
Initially, the nonhydroxylated S-C hybrids (1–7, Scheme 1) were synthesized via a sequential Claisen–Schmidt condensation between 4-iodo-/bromoacetophenone and various aromatic/heteroaromatic benzaldehydes followed by Heck coupling of the resulting iodo-/bromochalcones with styrene or *p*-chlorostyrene. In order to further expand the scope of the above hybrid molecules (1–7), the introduction of hydroxy

Scheme 2^a

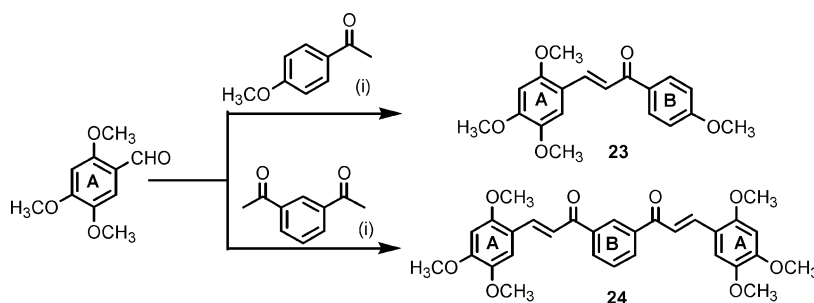
^aReagents and conditions: (i) NaOH, MeOH at room temp, 8 h; (ii) Pd(PPh₃)₄, DMF, piperidine, LiCl, reflux, 14 h.

Scheme 3^a

^aReagents and conditions: (i) dimethyl sulfate, K₂CO₃, acetone, reflux, 24 h; (ii) acetic anhydride, sodium acetate, DMAP, DMF at room temp, 3 h; (iii) *p*-toluenesulfonyl chloride, pyridine, cat. DMAP, DMF at room temp, 2 h; (iv) 3,5-dichlorobenzenesulfonyl chloride, pyridine, cat. DMAP, DMF at room temp, 2 h.

Scheme 4^a

^aReagents and conditions: (i) Pd(PPh₃)₄, DMF, piperidine, LiCl, reflux, 14 h.

Scheme 5^a

^aReagents and conditions: (i) NaOH, MeOH at room temp, 8 h.

substitution at the stilbene ring was envisaged, as such functional groups are known to impart enhanced biological activities.⁹ In this context, the Heck coupling of iodochalcone with hydroxystyrene seemed an attractive synthetic route. However, the hydroxystyrenes are known to be prone to polymerization and many of them, e.g., canolol (4-hydroxy-3,5-dimethoxystyrene), are also not commercially available. Therefore, it was decided to undertake in situ synthesis of hydroxy substituted styrenes using our¹¹ modified Knoevenagel

decarboxylation approach followed by their Heck coupling with iodochalcones in the same pot. As illustrated in Scheme 1, the above methodology was found to be quite useful for the synthesis of diverse hydroxy substituted stilbene–chalcone hybrids (8–13) from readily available benzaldehydes. The above success encouraged us to explore a one-pot Claisen–Schmidt/Knoevenagel–decarboxylation–Heck coupling sequence; however, the desired product (11) was obtained in comparatively lower yield (10%) compared to 33% (in the case

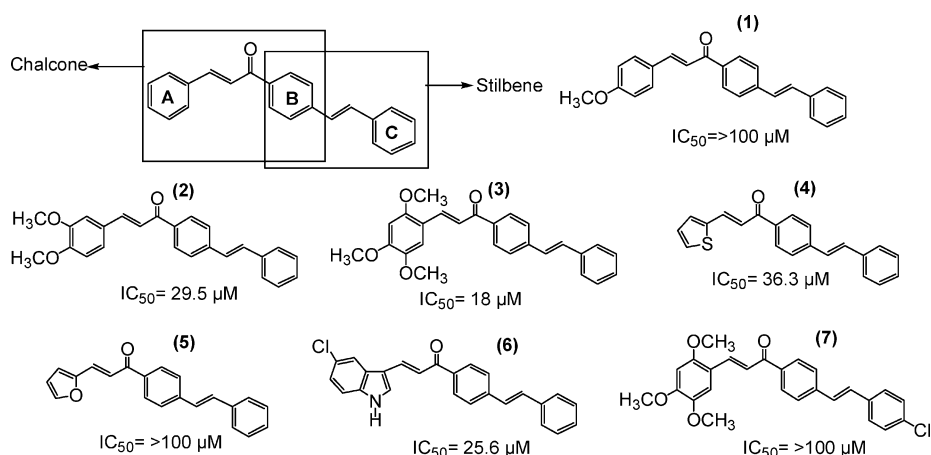


Figure 3. Antimalarial profile of nonhydroxylated stilbene–chalcone hybrids.

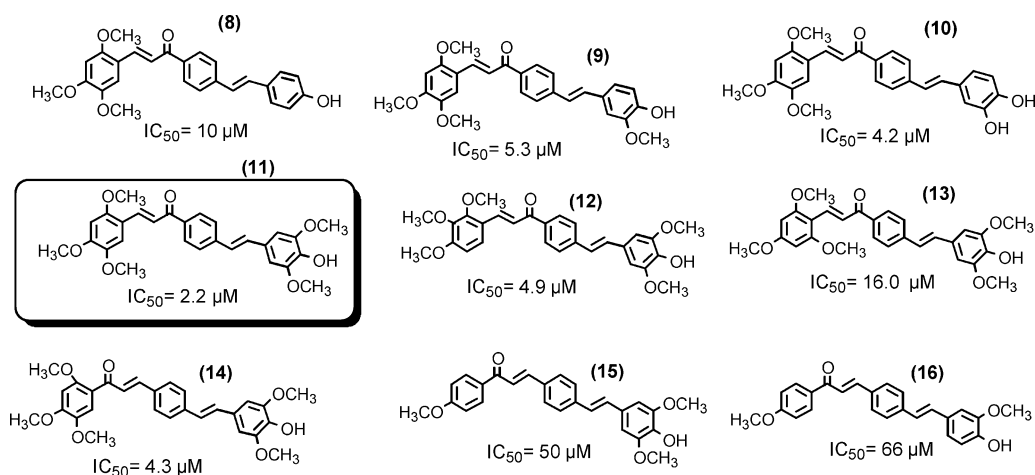


Figure 4. In vitro antimalarial potency of S-C hybrid derivatives against *P. falciparum* 3D7.

of two-step synthesis of **11**) (see Supporting Information for details).

Interestingly, this approach developed for hybrid molecules (**8–13**, A–HC=CH–CO–B) was also successfully applied for the synthesis of stilbene–chalcone hybrids possessing reverse arrangement of the α,β -unsaturated carbonyl group (A–CO–HC=CH–B) across the rings A and B via condensation between 4-iodobenzaldehyde and substituted acetophenones followed by Heck coupling (**14–16**, Scheme 2).

In order to introduce further diversity in the S-C hybrids synthesized as above, the hydroxy substitution on compound **11** was modified into methylated and acetylated^{12a} derivatives (**17** and **18**, Scheme 3). Similarly, sulfonyl derivatives^{12b,c} of **11** were prepared using *p*-toluenesulfonyl chloride and 3,5-dichlorobenzenesulfonyl chloride (**19** and **20**, Scheme 3) in DMF at room temperature.

On the other hand, the hydroxystilbene **21** and distyrylbenzene **22** (Scheme 4) were synthesized via our earlier reported palladium catalyzed domino Knoevenagel–Heck reaction^{11c} between the appropriate hydroxybenzaldehyde, malonic acid, and haloarenes.

Similarly **23** (chalcone) and **24**, a bis-chalcone (Scheme 5), were synthesized via condensation between 2,4,5-trimethoxybenzaldehyde and *p*-methoxyacetophenone or 1,3-diacetylbenzene, respectively.

All the synthesized compounds were fully characterized by ¹H and ¹³C NMR and further confirmed through HRMS analysis.

Antiplasmodial Activity and Structure–Activity Relationships. The stilbene–chalcone hybrid compounds synthesized as above were screened for in vitro antimalarial potency against *Pf* 3D7 (CQ sensitive *Plasmodium falciparum* strain) using microtiter based SYBR Green I fluorescence assay.¹³ Initially, the nonhydroxylated S-C hybrids (Figure 3, **1–7**) were screened against *Pf* 3D7. The rings B and C were kept constant, while the substitution on ring A was varied.

It is evident from Figure 3 that a progressive increase in electron density on ring A resulted in progressive enhancement in antiplasmodial potency, with the 2,4,5-trimethoxy substituted S-C hybrid (**3**) displaying the most promising activity ($IC_{50} = 18 \mu M$) followed by dimethoxy (**2**, $IC_{50} = 29.5 \mu M$) and monomethoxy (**1**, $IC_{50} > 100 \mu M$). On the other hand, the replacement of ring A with heteroaromatic moieties like thiophene, furan, and indole (Figure 3, **4–6**) led to only moderate activities (IC_{50} of 36.3, >100, and 25.6 μM , respectively). Having realized the importance of electron releasing groups on ring A, we retained the 2,4,5-trimethoxy substitution pattern while probing further structure–activity relationship (SAR) studies. To begin with, we decided to evaluate the antiplasmodial effect of structural variations on ring C of the S-C hybrids. The presence of an electron

withdrawing (*p*-Cl) group on ring C resulted in loss of activity (Figure 3, 7, $IC_{50} > 100 \mu M$). In view of the immense pharmacological importance of hydroxy substituted stilbenes,¹⁴ we were inspired to evaluate the antimalarial profiles of various S-C hybrids possessing a hydroxylated C ring. Gratifyingly, our above premise was confirmed, as the hydroxy S-C hybrids (Figure 4) were in general found to display comparatively enhanced potency with antimalarial activity, progressively increasing upon an increase in electron density at ring C, (8, 9, 10, and 11 with IC_{50} of 10, 5.3, 4.2, and 2.2 μM , respectively). In particular, 11, possessing high electron density in both rings A and C, showed the best antimalarial activity ($IC_{50} = 2.2 \mu M$) against the Pf3D7 strain. Further the declining potency in trimethoxy positional isomers 12 ($IC_{50} = 4.9 \mu M$) and 13 ($IC_{50} = 16 \mu M$) indicated the importance of 2,4,5-trimethoxy substitution on ring A (11) for the most potent antimalarial effect.

In order to discern the role of relative positions of rings A and B in the above scaffolds (A–C=CH–CO–B), the S-C hybrids possessing chalcone moiety with reversal in rings A and B (A–CO–HC=C–B) were also evaluated for antiplasmodial activity (Figure 4, 14–16). Interestingly, such a study revealed the beneficial role of the presence of a strong electron withdrawing (carbonyl) group adjacent to the stilbene moiety, as the S-C hybrids possessing an exocyclic olefinic bond adjacent to the stilbene moiety generally displayed lower activity, with 14 possessing an IC_{50} of 4.3 μM compared to 11 ($IC_{50} = 2.2 \mu M$). The above observation was further reinforced when 15' and 16' (isomers of 15 and 16, respectively, synthesized by a similar procedure as given in Scheme 1), possessing carbonyl group adjacent to the B ring, displayed higher potency (IC_{50} of 15 and 34 μM , respectively; Figure 5) in comparison to 15 and 16 (IC_{50} pf 50 and 66 μM , respectively; Figure 4).

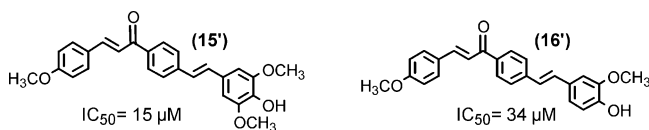
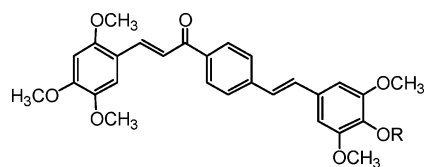


Figure 5. In vitro antimalarial potency of positional isomers of 15 and 16.

Having identified the core framework of an S-C hybrid (11) responsible for potent antiplasmodial activity, we were encouraged to evaluate the effect of further diversification on the above motif by installing various functional groups on the hydroxyl group of 11 (Figure 6, 17–20). However, methylation of hydroxy group in 11 led to decreased activity (17, $IC_{50} = 5.2 \mu M$), while acetylation (18, $IC_{50} = 2.2 \mu M$) caused no change in potency (Figure 6). On the other hand, the derivatization of 11 into *p*-tolylsulfonyl analogues resulted in drastically reduced antimalarial activity (19, 20; $IC_{50} > 100 \mu M$). Since progressive increments in the number of electron donating methoxy groups on rings A and C led to molecules with progressively increasing antimalarial potency, it is apparent that electron density in rings A and C is a determinant of antimalarial potency of S-C hybrids.

Finally, some of the potent hybrid compounds from the above series (with IC_{50} ranging from 2.2 to 5.2 μM against CQ sensitive Pf 3D7 strain) were screened for their antimalarial potency against two CQ resistant strains (Pf Dd2 and Pf INDO) {Table 1, Supporting Information (Figure 1)}. We



R in 17 = CH ₃	$IC_{50} = 5.2 \mu M$
18 = COCH ₃	$IC_{50} = 2.2 \mu M$
19 = SO ₂ C ₆ H ₄ CH ₃	$IC_{50} = >100 \mu M$
20 = SO ₂ C ₆ H ₃ Cl ₂	$IC_{50} = >100 \mu M$

Figure 6. Antimalarial activity of various derivatives of the most potent S-C hybrid 11.

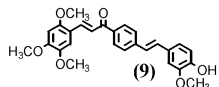
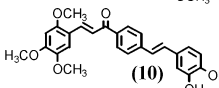
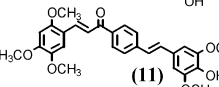
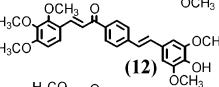
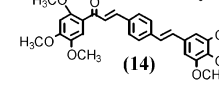
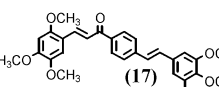
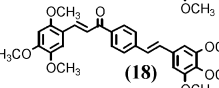
have observed that several S-C hybrids exhibited stronger antimalarial activity against CQ resistant than CQ sensitive strain of *Plasmodium falciparum*, giving resistance indices less than 1 (Table 1). Significantly, the most active S-C hybrid (11) that displayed $IC_{50} = 2.2 \mu M$ against Pf 3D7 displayed better potency against the *Plasmodium falciparum* CQ resistant strain (INDO, $IC_{50} = 1.4 \mu M$) with a resistance index of 0.64 (Table 1). Similarly, 11 was also found to be active against another Pf CQ resistant strain (Dd2, $IC_{50} = 6.4 \mu M$, resistance index of 2.9).

In addition, the active compounds were analyzed for their cytotoxic behavior against two mammalian cell lines, viz., HeLa and fibroblast L929. Therapeutic indices {TI = [IC_{50} (HeLa) or IC_{50} (L929)]/ IC_{50} (Pf3D7)} with values from 4.7 to >46.5 indicated that the most active compounds 11 and 18 (TI > 42 for HeLa and L929) were also relatively nontoxic.

In order to ascertain the specific benefit of merged stilbene–chalcone hybrid, the respective individual stilbene (4-hydroxy-3,4',5-trimethoxystilbene, 21), chalcone (1-(4-methoxyphenyl)-3-(2,4,5-trimethoxyphenyl)prop-2-en-1-one, 23), and their equimolar mixture were screened for antimalarial activity (Figure 7). In addition, some related scaffolds like dimeric stilbene (22) and dimeric chalcone (24) were also tested to evaluate the effect of extended conjugation. Significantly, both the individual stilbene/chalcone 21/23 ($IC_{50} > 100 \mu M/11.5 \mu M$) and the equimolar mixture of chalcone and stilbene ($IC_{50} = 32.5 \mu M$) displayed significantly decreased potency against *Plasmodium falciparum*, thereby demonstrating the significance¹⁵ of hybridized S-C scaffold (11) for antimalarial activity. Moreover, the 4-hydroxy analogue of chalcone 23, i.e., 1-(4-hydroxyphenyl)-3-(2,4,5-trimethoxyphenyl)prop-2-en-1-one (25; see Supporting Information), was found to be less potent ($IC_{50} = 61 \mu M$) than both 11 and 23, thereby suggesting that a 4-OH substitution has a potentiating effect on S-C hybrid but an opposite effect on chalcone. Interestingly, the distyrylbenzene 22 ($IC_{50} = 11.0 \mu M$) also turned out to be inactive, while $IC_{50} = 2.8 \mu M$ for bischalcone (24) suggests it to be nearly equipotent to the S-C hybrid (11). It is pertinent to mention that the S-C hybrid (11) represents a more promising scaffold over bis-chalcone (24), since the probability of resistance against homodimeric pharmacophores is likely to be higher than is the case with hybrid pharmacophores.

Mechanistic Studies. In spite of some suggestions that chalcones may target plasmodial proteases^{16,17} or cyclins,¹⁸ our knowledge of the antimalarial targets of chalcones is incomplete. The knowledge about mechanistic details of their antimalarial action is also minimal. Here we have attempted to

Table 1. Antimalarial and Antifalcipain Potency, Resistance, and Therapeutic Indices of Potent Stilbene–Chalcone Hybrids

Compound	SYBR green assay IC ₅₀ (μ M)			Resistance Index		Therapeutic Index		Falcipain-2 IC ₅₀ (μ M)
	Pf3D7	PfIndo	PfDd2	IC ₅₀ INDO/ IC ₅₀ 3D7	IC ₅₀ Dd2/ IC ₅₀ 3D7	IC ₅₀ HeLa/ IC ₅₀ 3D7	IC ₅₀ L929/ IC ₅₀ 3D7	
 (9)	5.3	2.65	3.71	0.5	0.7	>37.7	4.7	23.0
 (10)	4.2	4.6	7.1	1.1	1.7	>23.8	7.6	19.0
 (11)	2.2	1.4	6.4	0.64	2.9	42.3	45.5	37.5
 (12)	4.9	5.88	5.39	1.2	1.1	>43	>43	70.0
 (14)	4.3	2.58	3.01	0.6	0.7	>46.5	8.4	100.0
 (17)	5.2	2.08	2.6	0.4	0.5	>38.5	29.8	20.5
 (18)	2.2	1.98	2.2	0.9	1.0	>45.5	>45.5	25.0
Chloroquine	40 nM	500 nM	172 nM	12.5	4.3	>200	>200	ND

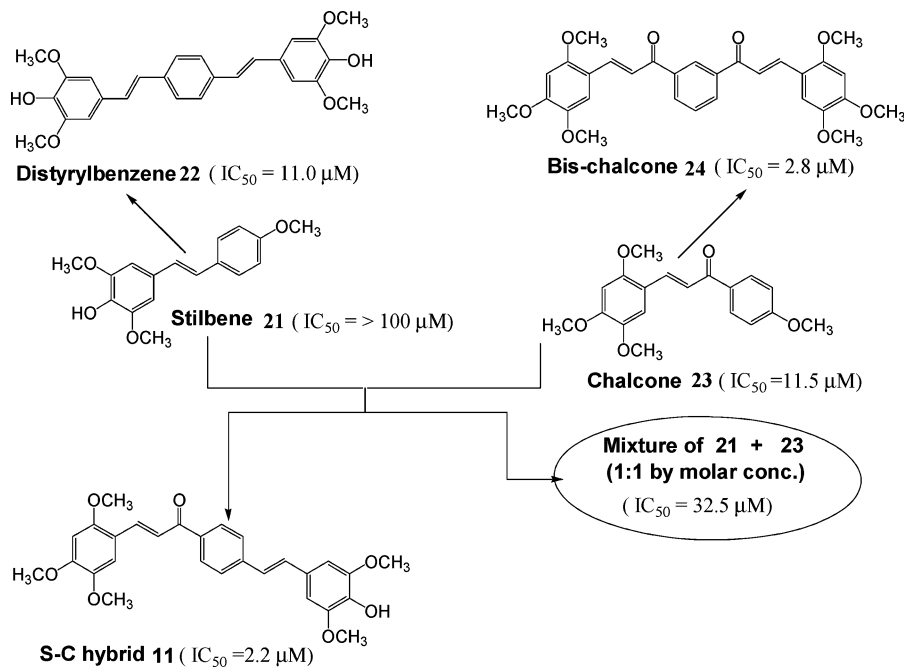


Figure 7. Antimalarial potency of S-C hybrid (11) compared to potencies of their individual components (21 and 23), homodimers (22 and 24), and equimolar mixture of stilbene and chalcone.

study the mechanism of antimalarial action of two S-C hybrids (11 and 18), found to be the most potent in the series of compounds studied by us. Microscopy based stage specificity experiments, where each of the stages of the parasite life cycle was treated with drugs, have indicated that 11 and 18 were specific for ring and trophozoite stage parasites and did not affect the schizont stage, egress of merozoites, or the process of merozoite invasion (Figure 8A). These microscopy based

results, which found confirmation also from the SYBR Green fluorescence assay (Figure 8B), suggest that some molecular targets common to ring and trophozoite stages may be involved in the antimalarial properties of S-C hybrids.

For instance, falcipain-2, a cysteine protease involved in hemoglobin degradation pathway of *P. falciparum*, is found in both rings and trophozoites¹⁹ and some early studies have reported that chalcones and their derivatives target the

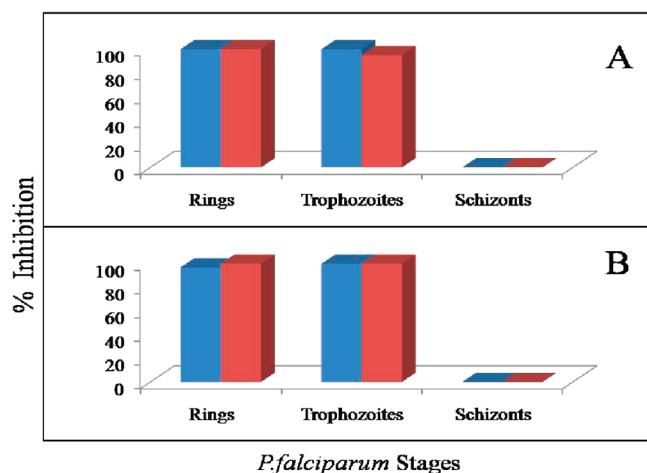


Figure 8. Specificity of **11** and **18** for rings and trophozoites. Highly synchronized stage enriched *Pf* 3D7 cultures were treated with IC_{100} values of each compound (**11**, $6 \mu\text{M}$; **18**, $10 \mu\text{M}$) for 48 h (rings), 24 h (trophozoites), and 8 h (schizonts). The parasites were washed with RPMI to remove the drug pressure and incubated for 48 h with drug free media. The percentages of inhibition of growth were determined by Giemsa staining (A) and fluorescence based SYBR Green I assay (B). Blue and red bars indicate effects of **11** and **18**, respectively. The inability of **11** and **18** to inhibit schizont stage progression indicates that they do not affect either egress of merozoites or their ability to invade healthy red cells.

hemoglobin degradation pathway by inhibiting falcipain-2.¹⁶ In order to find if falcipain-2 may be a target for the antimalarial action of S-C hybrids, we examined anti-falcipain-2 potency of all those hybrids whose antimalarial IC_{50} was $\leq 10 \mu\text{M}$. The enzyme inhibitory data of the potent compounds against falcipain-2 activity {Table 1, Supporting Information (Figure 2)} indicate that compounds **11** and **18** with antimalarial IC_{50} of $2.2 \mu\text{M}$ exhibit anti-falcipain-2 IC_{50} values of 37.5 and $25 \mu\text{M}$, respectively. The generally high IC_{50} values (19 – $100 \mu\text{M}$) of S-C hybrids against falcipain-2 and lack of a direct relation between anti-falcipain-2 potency and antimalarial potency suggest that the true targets of S-C hybrids may be different from falcipain 2. Similarly Dominguez et al.²⁰ also reported that the hybrid quinolinylchalcones failed to inhibit the falcipain-2 activity ($IC_{50} > 100 \mu\text{M}$) even as they inhibited the growth of the malaria parasite with an $IC_{50} \sim 1 \mu\text{M}$.

To find the activity of compounds against egress and invasion of *P. falciparum* at blood stage, **11** ($6 \mu\text{M}$) and **18** ($10 \mu\text{M}$) were incubated for 8 h with schizont stage parasites. As shown in Figure 9, **11** and **18** failed to inhibit schizont growth, merozoite egress, or RBC invasion. Hence, we predicted that in a continuous culture starting with schizonts, continuous drug pressure for an additional 48 h should stall growth of parasite at ring stage while the culture subjected to drug pressure for only 8 h followed by drug withdrawal during the 48 h time window must grow to the same extent as the untreated control culture. This was indeed found to be the case as shown by results in Figure 9 suggesting that schizonts, egress of merozoites, and their ability to invade fresh red blood cells are unaffected while rings are very sensitive to the action of **11** and **18**.

Studies on kinetics of action of **11** and **18** on ring stage parasites suggest that **11**, which caused complete inhibition of growth at 48 h, was slower in action than **18**, which caused similar inhibition of growth at 24 h (Figure 10A). However, in an analogous experiment with trophozoite stage parasite culture

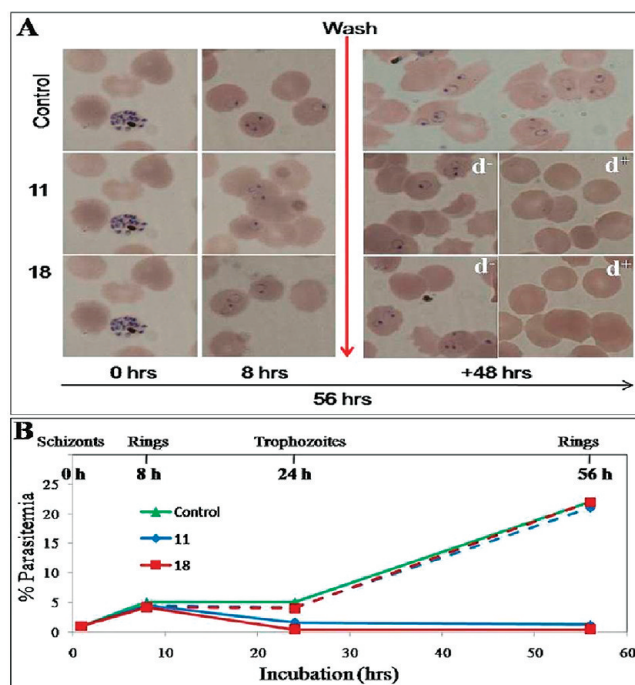


Figure 9. Schizonts treated with **11/18** are trapped at ring stage. (A) Highly synchronized schizont stage *Pf* 3D7 cultures were grown without (control) or with test compounds at their respective IC_{100} (**11**, $6 \mu\text{M}$, middle panel; **18**, $10 \mu\text{M}$, bottom panel). All cultures were washed free of drug using cRPMI after 8 h. The drug treated cultures were further incubated with drug free (d^-) or drug supplemented (d^+) complete RPMI for an additional 48 h. Cultures were Giemsa stained and microscopically examined for parasitemia and stage of growth. Note that 8 h of drug exposure causes no effect on the transition of schizont to ring stage. However, reincubation with drug causes arrest at ring stage. (B) Quantitative microscopic data obtained using auto count have been plotted to show that schizont progression to rings is unaffected by the presence of drug for 8 h. Continuous drug exposure (solid lines) versus 8 h of drug exposure (first time window) followed by drug withdrawal and growth for 48 h (second time window) in drug free RPMI (dotted lines) indicates that in the presence of drug the schizont successfully transits to ring stage and parasitemia increases steadily (in the absence of drug beyond 8 h) but rings are killed when the drug is present in the second time window.

(Figure 10B), **11**, which caused complete inhibition of growth at 18 h, was found to be faster acting than **18**, which caused similar growth inhibition only at 24 h.

Apoptosis, a well-known programmed cell death (PCD) mechanism in multicellular organisms, is not well studied in unicellular organisms.^{21,22} But recent studies have revealed that unicellular organisms like leishmania, yeast, bacteria, blastocystis, trypanosomes, and trichomonas also undergo PCD and show apoptotic features resembling multicellular organisms.^{23,24} Thus, Picot et al.²⁵ reported chloroquine induced oligonucleosomal DNA fragmentation suggesting PCD in nonsynchronized erythrocytic stages of CQ sensitive *P. falciparum* strain. Recent studies have reported that CQ, etoposide (topoisomerase II inhibitor), and staurosporine (protein kinase C inhibitor) induced PCD in CQ sensitive and resistant strains of *P. falciparum* with hallmark features of apoptosis including nuclear chromatin condensation, DNA fragmentation, loss of mitochondrial membrane potential, and changes in plasma membrane permeability.^{26–28} Lopez et al.²⁹ described that the trophozoite and schizont stage-specific antimalarial *Solanum*

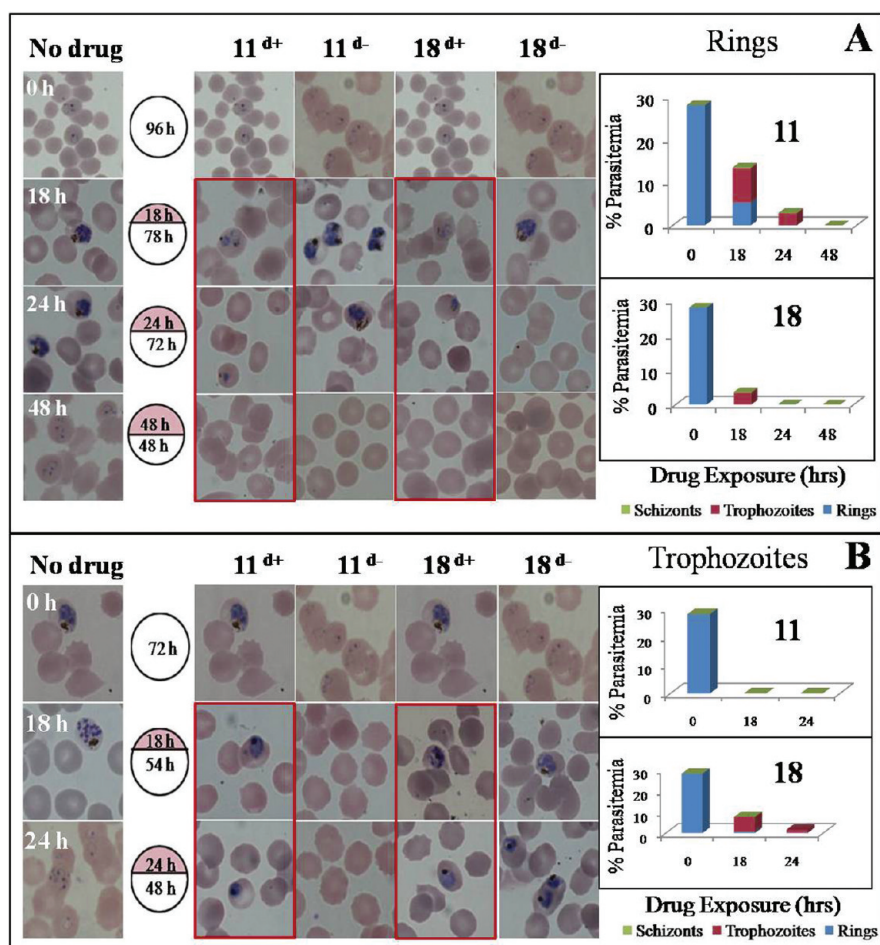


Figure 10. Microscopic examination of the effect of exposure of **11** and **18** (each at its IC_{100}) for variable time durations to ring and trophozoite stages. Synchronized cultures of *P. falciparum* 3D7 were incubated with IC_{100} of **11** ($6 \mu M$) and **18** ($10 \mu M$) for different time periods (d^+ , solid red boundaries) followed by transition to drug free medium (d^-). Total incubations (with and without drug pressure) for ring and trophozoite stages were 96 and 72 h, respectively. In circles on the left margin, colored and colorless sections represent periods of drug and drug free exposures, respectively.

nudum steroids induced PCD in *P. falciparum* with features of apoptosis. The finding of a putative *P. falciparum* metacaspase (*Pf* MCA-1)²⁸ has provided further support for the occurrence of PCD in *P. falciparum*. However, Nyakeriga et al.³⁰ have reported that chloroquine, atovaquone, and etoposide treatments caused nonapoptotic cell death because these agents failed to show any features of apoptosis. Likewise, another report suggested that CQ and *S*-nitroso-*N*-acetylpenicillamine (SNAP) treated blood stage *P. falciparum* died by autophagic-like cell death without display of any apoptotic features.³¹ Metazoan apoptotic features including chromatin condensation, nuclear DNA fragmentation, movement of phosphatidylserine from the inner to the outer lamellae of the cell membrane, and caspase-like protein activity have been observed in mosquito midgut stage parasite of *P. berghei* (ookinete) both in vivo and in vitro.^{32,33} Against this background, in the present study, we have found that compounds **11** and **18** at their respective IC_{100} caused apoptotic cell death in *P. falciparum* 3D7 strain. To the best of our knowledge, this is the first report of apoptotic cell death caused by stilbene–chalcone hybrids in *P. falciparum*. Treated parasites showed features of apoptotic cell death including cell shrinkage, chromatin condensation, DNA fragmentation, and loss of mitochondrial membrane potential (Figure 11). Ring and trophozoite stage parasites treated with

11/18 showed crisis forms with condensed nuclei at 24 and 18 h, respectively, and the resulting reduction in parasitemia at 48 h (Figure 11). DNA fragmentation or degradation is one of the major features of apoptosis.³⁴ Hoescht 33342 staining²⁹ further confirmed the nuclear morphological changes including chromatin condensation and fragmentation in *P. falciparum*. Indeed the results of Hoescht 33342 staining also showed distinct nuclear condensation in both ring and trophozoite stage parasites at 18 h. Similar observations have earlier been made by Lopez et al. and Meslin et al.^{28,29} At a later time point (24 h), we observed clear internucleosomal fragmentation in trophozoite stage parasites but not in ring stage parasites. This may be due to the small size of nucleus in rings vs a significantly larger nucleus in trophozoites. It is not clear why internucleosomal fragmentation so clearly visible in Hoescht 33342 staining was not apparent in Giemsa staining (Figure 11). The loss of mitochondrial membrane potential ($\Delta\Psi_m$) of ring and trophozoite stage *P. falciparum* similar to CQ, atovaquone, etoposide,²⁸ and *Solanum nudum* steroids.²⁹ The results of JC-1 staining indicative of loss of $\Delta\Psi_m$ displayed strong evidence of apoptosis in *P. falciparum* by S-C hybrids. Thus, our data have shown high percentage of

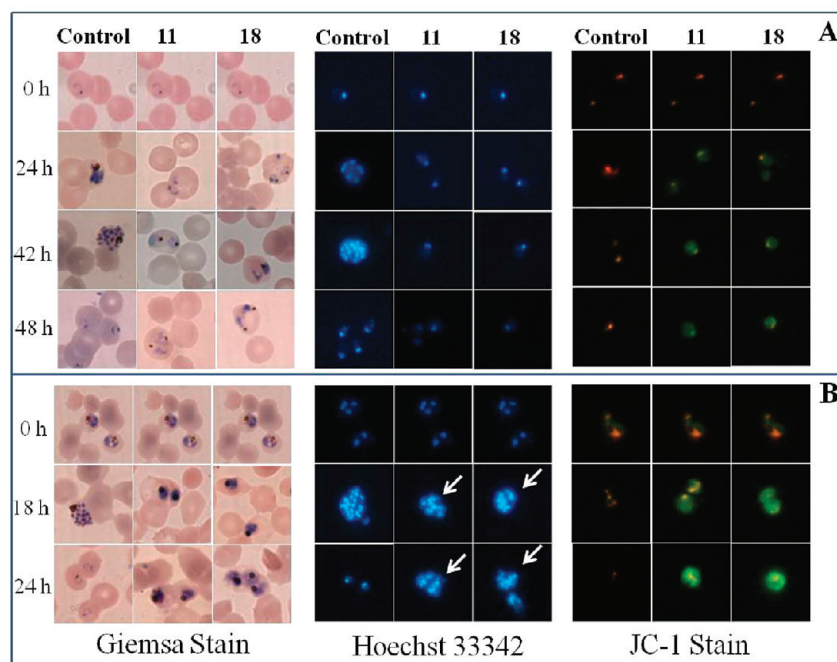


Figure 11. Induction of apoptosis in *P. falciparum* by S-C hybrids. S-C-hybrid-treated erythrocyte stage parasites showed features of apoptosis including chromatin condensation/DNA fragmentation and loss of mitochondrial membrane potential ($\Delta\Psi_m$). Panels A and B show the effects of **11** ($6\ \mu\text{M}$) and **18** ($10\ \mu\text{M}$) at different time points on the ring and trophozoite stage parasites, respectively. DNA degradation was observed in both **11** and **18** treated ring and trophozoite parasites by Giemsa staining. The arrow marks show the DNA fragmentation in trophozoite stage parasites treated with **11** and **18** by Hoechst 33342 staining. The loss of mitochondrial membrane potential was monitored by JC-1 stain. High $\Delta\Psi_m$ in control mitochondria causes association with the dye in an aggregated state leading to red-orange fluorescence emission. **11** and **18** treated parasites lead to dissipation of $\Delta\Psi_m$, and the dye is now partitioned into cytosol, resulting in green fluorescence.

chromatin condensation, nucleus fragmentation, and loss of $\Delta\Psi_m$ in S-C hybrids treated parasites. The high therapeutic indices (>45) of **11** and **18** suggest that these compounds may gain specificity by choosing to specifically target the apoptotic machinery of the malaria parasite. The above results assume significance, as apoptotic plasmodium cell death has been recognized to be a novel and promising target for developing newer antimalarials.^{26,35}

CONCLUSION

We have for the first time hybridized the hydroxystilbene and chalcone pharmacophores through a facile Claisen–Schmidt/Knoevenagel–decarboxylation/Heck approach. Significantly, the obtained hybrid compounds were found to provide a new and promising class of antimalarial agents against CQ resistant strains of *P. falciparum*. The SAR analysis revealed that a 2,4,5-trimethoxy substitution on ring A and 4-hydroxy-3,5-dimethoxy substitution on ring C were critical for the stilbene–chalcone hybrids to display potent antiplasmodial activity. We have found these hybrids to have promising resistance and therapeutic indices. Further, our data suggest that (a) the S-C hybrids are far more potent than the physical mixture of the constituent pharmacophores, (b) the antimalarial activity of S-C hybrids may not be due to inhibition of falcipain-2, and (c) S-C hybrids cause stage-specific death resembling apoptosis in rings and trophozoites without perturbing the progression of schizonts into rings. The observation that S-C hybrids caused signs of programmed cell death in *Plasmodium* is significant, since it suggests Plasmodium-specific new drug targets for this class of molecules. Moreover, the above S-C hybrids also displayed low cytotoxicities, thereby opening the possibility of

modifying the lead candidates into clinically useful antimalarial compounds.

EXPERIMENTAL SECTION

Materials and Methods. All the starting materials were reagent grade. The palladium catalysts were purchased from Acros, Aldrich, and Merck and used as such. The substituted benzaldehydes, acetophenones, and all other reagents were obtained from commercial sources (Merck, Lancaster). The solvents used for isolation/purification of compounds were obtained from commercial sources (Merck) and used without further purification. Column chromatography was performed using silica gel (Merck, 60–120 mesh size). The chromatographic solvents are mentioned as v/v ratios. All the synthesized compounds were fully characterized by ^1H and ^{13}C NMR and further confirmed through HRMS analysis. ^1H (300 MHz), ^{13}C (75.4 MHz), and two-dimensional NMR spectra were recorded on a Bruker Avance-300 spectrometer. The following abbreviations were used to designate chemical shift multiplicities: s = singlet, d = doublet, t = triplet, m = multiplet, q = quartet. The ^{13}C NMR spectra are proton decoupled. The melting points were determined on a digital Barnsted Electrothermal 9100 apparatus and are uncorrected. HRMS-ESI spectra were determined using micromass Q-TOF Ultima spectrometer and reported as m/z (relative intensity). The purity of the test compounds was determined by HPLC analysis using a Shimadzu LC-20 instrument equipped with a photodiode array detector (CBM 20A) and a Purospher-Star RP-18e column (4.6 mm \times 150 mm, 5 μm , Merck). Methanol–acetonitrile (70:30, v/v) (solvent A) and TFA (0.05%) (solvent B) were used as mobile phases. The above analysis indicated purity of $\geq 95\%$.

Representative Procedure for the Synthesis of Stilbene–Chalcone Hybrid 1 via Claisen–Schmidt Condensation–Heck Coupling Reaction (Scheme 1 and Figure 3). To a solution of 4-iodoacetophenone (3.2 mmol) in methanol (15 mL) were added 10% aqueous NaOH (6 mmol) and *p*-methoxybenzaldehyde (0.4 g, 3 mmol). The reaction mixture was stirred until complete consumption

of starting material. The methanol was evaporated from the above mixture, and the obtained precipitates were washed with dilute HCl, excess water, dried in air, and finally recrystallized with methanol to obtain pure 4-iodo-4'-methoxychalcone (0.85 g, yield 80%).

In the second step, to the solution of 4-iodo-4'-methoxychalcone (0.5 g, 1.18 mmol) and styrene (1.88 mmol) in DMF (20 mL) were added piperidine (1.18 mmol), Pd(PPh₃)₄ (0.035 mmol), and LiCl (0.09 mmol). Then the mixture was refluxed for 14 h (until the completion of reaction). The above mixture was cooled to room temperature and filtered through Celite. The filtrate was poured into water (100 mL, acidified with dilute HCl, pH 5–6) and extracted with ethyl acetate (2 × 40 mL). The combined organic layer was washed with water (2 × 15 mL), brine (1 × 10 mL), dried over Na₂SO₄, and vacuum evaporated. The residue was subsequently purified by column chromatography on silica gel (60–120 mesh size) using hexane/ethyl acetate (9.3:0.7) to give product 1.

(2E)-1-{4-[(E)-2-Phenylethenyl]phenyl}-3-(4-methoxyphenyl)prop-2-en-1-one (1). Cream solid (48% yield); mp 162–164 °C; ¹H NMR (CDCl₃, 300 MHz), δ (ppm) 8.06 (2H, d, J = 8.3 Hz), 7.86 (1H, d, J = 15.6 Hz), 7.65 (4H, d, J = 8.3 Hz), 7.56 (2H, d, J = 7.3 Hz), 7.49 (1H, d, J = 15.6 Hz), 7.38 (1H, d, J = 7.6 Hz), 7.34 (1H, d, J = 7.3 Hz), 7.27 (3H, q), 6.98 (2H, d, J = 8.1 Hz), 3.88 (3H, s); ¹³C NMR (75.4 MHz, CDCl₃), δ (ppm) 189.9, 162.1, 144.9, 142.0, 137.7, 137.2, 131.7, 130.7, 129.4, 129.2, 128.7, 128.1, 128.0, 127.2, 127.0, 120.0, 114.8, and 55.8. HRMS-ESI: *m/z* [M + H]⁺ for C₂₄H₂₀O₂, calculated 341.1536; observed 341.1541.

Synthesis of Other Stilbene–Chalcone Hybrids 2–7 (Scheme 1 and Figure 3). The above procedure was followed.

(2E)-1-{4-[(E)-2-Phenylethenyl]phenyl}-3-(3,4-dimethoxyphenyl)prop-2-en-1-one (2). Yellow solid (44% yield); mp 147–149 °C; ¹H NMR (CDCl₃, 300 MHz), δ (ppm) 8.06 (2H, d, J = 8.1 Hz), 7.83 (1H, d, J = 15.6 Hz), 7.65 (2H, d, J = 8.1 Hz), 7.57 (2H, d, J = 7.6 Hz), 7.46 (1H, d, J = 15.6 Hz), 7.42 (2H, t, J = 7.4 Hz), 7.34 (1H, d, J = 7.6 Hz), 7.28–7.24 (3H, m), 6.93 (1H, d, J = 8.1 Hz), 4.19 (1H, s), 3.97 (3H, s), 3.96 (3H, s); ¹³C NMR (75.4 MHz, CDCl₃), δ (ppm) 189.9, 151.8, 149.6, 145.2, 142.0, 137.6, 137.1, 131.7, 129.6, 129.2, 128.9, 128.8, 128.7, 128.0, 127.2, 127.0, 123.6, 111.5, 110.5, and 56.4. HRMS-ESI: *m/z* [M + H]⁺ for C₂₅H₂₂O₃, calculated 371.1641; observed 371.1622.

(2E)-1-{4-[(E)-2-Phenylethenyl]phenyl}-3-(2,4,5-trimethoxyphenyl)prop-2-en-1-one (3). Yellow solid (52% yield); mp 148–150 °C; ¹H NMR (CDCl₃, 300 MHz), δ (ppm) 8.16 (1H, d, J = 15.7 Hz), 8.06 (2H, d, J = 7.9 Hz), 7.66 (2H, d, J = 7.9 Hz), 7.59 (2H, t, J = 7.5 Hz), 7.48 (1H, d, J = 15.7 Hz), 7.41 (2H, d, J = 7.5 Hz), 7.38 (1H, d, J = 7.1 Hz), 7.32 (1H, d, J = 7.5 Hz), 7.20 (2H, d, J = 10.9 Hz), 6.55 (1H, s), 3.97 (3H, s), 3.93 (6H, s); ¹³C NMR (75.4 MHz, CDCl₃), δ (ppm) 190.6, 155.1, 152.9, 143.7, 141.7, 140.4, 138.1, 137.2, 131.5, 129.4, 129.2, 128.6, 128.1, 127.2, 126.8, 120.7, 116.0, 111.9, 97.3, 57.0, 56.8, and 56.5. HRMS-ESI: *m/z* [M + H]⁺ for C₂₆H₂₄O₄, calculated 401.1747; observed 401.1721.

(2E)-1-{4-[(E)-2-Phenylethenyl]phenyl}-3-(thiophen-2-yl)prop-2-en-1-one (4). Yellow solid (46% yield); mp 138–140 °C; ¹H NMR (CDCl₃, 300 MHz), δ (ppm) 8.06–7.99 (2H, m), 7.96 (1H, s), 7.66 (2H, d, J = 8.9 Hz), 7.56 (2H, d, J = 7.2 Hz), 7.46 (1H, d, J = 7.2 Hz), 7.41–7.28 (5H, m), 7.25 (2H, d, J = 8.9 Hz), 7.14 (1H, q); ¹³C NMR (75.4 MHz, CDCl₃), δ (ppm) 189.0, 163.8, 147.7, 143.9, 140.0, 135.7, 134.4, 131.6, 131.2, 130.7, 129.3, 129.0, 127.1, 126.4, 121.7, 114.2, and 104.0. HRMS-ESI: *m/z* [M + H]⁺ for C₂₁H₁₆OS, calculated 317.0994; observed 317.0982.

(2E)-1-{4-[(E)-2-Phenylethenyl]phenyl}-3-(furan-2-yl)prop-2-en-1-one (5). Yellow solid (43% yield); mp 122–124 °C; ¹H NMR (CDCl₃, 300 MHz), δ (ppm) 8.08 (2H, d, J = 7.8 Hz), 7.66 (1H, s), 7.63–7.54 (5H, m), 7.43–7.38 (3H, t, J = 7.2 Hz), 7.35–7.30 (2H, m), 7.20 (1H, d, J = 16.3 Hz), 6.75 (1H, s), 6.55 (1H, s); ¹³C NMR (75.4 MHz, CDCl₃), δ (ppm) 189.3, 152.2, 145.3, 142.2, 137.4, 137.2, 131.8, 130.9, 129.4, 129.2, 128.7, 128.0, 127.2, 127.0, 119.6, 116.6, and 113.1. HRMS-ESI: *m/z* [M + H]⁺ for C₂₁H₁₆O₂, calculated 301.3659; observed 301.3650.

(2E)-1-{4-[(E)-2-Phenylethenyl]phenyl}-3-(5-chloro-1H-indol-3-yl)prop-2-en-1-one (6). Yellow solid (47% yield); mp 248–250

°C; ¹H NMR (CD₃COCD₃, 300 MHz), δ (ppm) 11.45 (1H, s), 8.07 (3H, d, J = 8.2 Hz), 7.92 (1H, s), 7.71 (3H, t, J = 7.2 Hz), 7.58–7.52 (3H, m), 7.47 (1H, d, J = 7.8 Hz), 7.41 (2H, t, J = 7.3 Hz), 7.32 (1H, d, J = 6.7 Hz), 7.24–7.15 (3H, m); ¹³C NMR (75.4 MHz, CDCl₃/DMSO, 9:1), δ (ppm) 188.7, 140.3, 137.7, 136.9, 135.9, 135.4, 131.6, 130.1, 127.9, 127.3, 126.8, 125.9, 125.7, 122.2, 118.9, 116.0, 112.8, and 112.2. HRMS-ESI: *m/z* [M + H]⁺ for C₂₅H₁₈ONCl, calculated 384.1149; observed 384.1129.

(2E)-1-{4-[(E)-2-(4-Chlorophenyl)ethenyl]phenyl}-3-(2,4,5-trimethoxyphenyl)prop-2-en-1-one (7). Yellow solid (35% yield); mp 118–120 °C; ¹H NMR (CDCl₃, 300 MHz), δ (ppm) 8.14 (1H, d, J = 15.7 Hz), 8.03 (4H, d, J = 7.9 Hz), 7.62 (1H, d, J = 7.9 Hz), 7.51–7.42 (3H, m), 7.35 (2H, d, J = 8.4 Hz), 7.12 (2H, d, J = 6.0 Hz), 6.53 (1H, s), 3.95 (3H, s), 3.91 (6H, s); ¹³C NMR (75.4 MHz, CDCl₃), δ (ppm) 180.0, 155.1, 153.0, 143.7, 141.3, 140.5, 135.7, 134.2, 130.6, 130.1, 129.5, 129.4, 129.0, 128.7, 128.3, 126.9, 120.6, 116.0, 111.9, 97.3, 57.0, 56.8, and 56.5. HRMS-ESI: *m/z* [M + H]⁺ for C₂₆H₂₃O₄Cl, calculated 435.1357; observed 435.1372.

Representative Procedure for the Synthesis of Hydroxyl Stilbene–Chalcone Hybrid 8 via Knoevenagel Condensation–Decarboxylation–Heck Sequence (Scheme 1 and Figure 4).

To a solution of 4-iodoacetophenone (3.2 mmol) in methanol (15 mL) were added 10% aqueous NaOH (6 mmol) and 2,4,5-trimethoxybenzaldehyde (3 mmol). The reaction mixture was stirred until complete consumption of starting material. The methanol was vacuum evaporated from above mixture, and the obtained precipitates were washed with dilute HCl, excess water, dried in air, and finally recrystallized with methanol to obtain pure substituted 4-iodochalcone. In the second step, to the stirred mixture of malonic acid (8.4 mmol) and piperidine (10.60 mmol) in DMF (20 mL) were added 4-hydroxybenzaldehyde (2.12 mmol), substituted 4-iodochalcone (0.5 g, 1.18 mmol), Pd(PPh₃)₄ (0.035 mmol), and LiCl¹⁸ (0.09 mmol), and the mixture was refluxed for 14 h. The above mixture was cooled to room temperature and filtered through Celite. The filtrate was poured into water (100 mL, acidified with dilute HCl, pH 5–6) and extracted with ethyl acetate (2 × 40 mL). The combined organic layer was washed with water (2 × 15 mL), brine (1 × 10 mL), dried over Na₂SO₄, and vacuum evaporated. The residue was subsequently purified by column chromatography on silica gel (60–120 mesh size) using hexane/ethyl acetate (9.3:0.7) to give product 8.

(2E)-1-{4-[(E)-2-(4-Hydroxyphenyl)ethenyl]phenyl}-3-(2,4,5-trimethoxyphenyl)prop-2-en-1-one (8). Reddish brown solid (30% yield); mp 78–80 °C; ¹H NMR (CD₃COCD₃, 300 MHz), δ (ppm) 8.15 (1H, d, J = 15.7 Hz), 8.03 (2H, d, J = 8.1 Hz), 7.60 (2H, d, J = 8.2 Hz), 7.53 (1H, d, J = 15.7 Hz), 7.44 (2H, d, J = 8.3 Hz), 7.15 (2H, s), 7.02 (1H, d, J = 16.3 Hz), 6.90 (2H, d, J = 8.3 Hz), 6.53 (1H, s), 3.95 (3H, s), 3.92 (6H, s); ¹³C NMR (75.4 MHz, CDCl₃), δ (ppm) 190.8, 157.3, 155.1, 152.9, 143.7, 142.4, 140.4, 137.5, 131.4, 129.5, 128.6, 126.5, 125.4, 120.6, 116.3, 116.0, 111.9, 97.3, 57.0, 56.8, and 56.5. HRMS-ESI: *m/z* [M + H]⁺ for C₂₆H₂₄O₅, calculated 417.1696; observed 417.1672.

Synthesis of Other Hydroxylated Stilbene–Chalcone Hybrids Including 9–13 (Scheme 1 and Figure 4). The above procedure was followed.

(2E)-1-{4-[(E)-2-(4-Hydroxy-3-methoxyphenyl)ethenyl]phenyl}-3-(2,4,5-trimethoxyphenyl)prop-2-en-1-one (9). Yellow solid (29% yield); mp 78–80 °C; ¹H NMR (CDCl₃, 300 MHz), δ (ppm) 8.15 (1H, d, J = 15.8 Hz), 8.03 (2H, d, J = 7.8 Hz), 7.60 (2H, d, J = 7.8 Hz), 7.52 (1H, d, J = 15.8 Hz), 7.19–7.01 (5H, m), 6.96 (1H, t, J = 5.2 Hz), 6.52 (1H, s), 5.84 (1H, s), 3.95 (6H, s), 3.90 (6H, s); ¹³C NMR (75.4 MHz, CDCl₃), δ (ppm) 190.6, 155.1, 152.9, 147.2, 146.6, 143.7, 142.1, 140.3, 137.6, 131.5, 129.9, 129.4, 126.6, 125.8, 121.4, 120.6, 116.0, 115.1, 111.9, 108.9, 97.3, 57.0, 56.8, 56.5, and 56.3. HRMS-ESI: *m/z* [M + H]⁺ for C₂₇H₂₆O₆, calculated 447.1802; observed 447.1816.

(2E)-1-{4-[(E)-2-(3,4-Dihydroxyphenyl)ethenyl]phenyl}-3-(2,4,5-trimethoxyphenyl)prop-2-en-1-one (10). Light orange solid (24% yield); mp 121–123 °C; ¹H NMR (CD₃COCD₃, 300 MHz), δ (ppm) 8.21 (2H, d, J = 15.7 Hz), 8.12 (2H, d, J = 8.2 Hz), 8.03 (1H, s), 7.80 (1H, d, J = 15.7 Hz), 7.72 (2H, d, J = 8.2 Hz), 7.50 (1H, s), 7.33 (1H, d, J = 16.4 Hz), 7.13 (1H, d, J = 16.4 Hz), 7.03 (2H,

q), 6.88 (1H, d, $J = 8.2$ Hz), 6.81 (1H, s), 3.96 (3H, s), 3.94 (3H, s), 3.86 (3H, s); ^{13}C NMR (75.4 MHz, CD_3COCD_3), δ (ppm) 189.6, 156.1, 154.8, 147.3, 146.7, 145.1, 143.5, 140.0, 138.5, 132.8, 130.8, 130.2, 127.5, 126.0, 121.1, 120.5, 116.8, 116.6, 114.6, 113.1, 98.8, 57.5, 57.3, and 56.8. HRMS-ESI: m/z $[\text{M} + \text{H}]^+$ for $\text{C}_{26}\text{H}_{24}\text{O}_6$, calculated 433.1645; observed 433.1621.

(2E)-1-[4-[(E)-2-(4-Hydroxy-3,5-dimethoxyphenyl)ethenyl]phenyl]-3-(2,4,5-trimethoxyphenyl)prop-2-en-1-one (11). Brownish yellow solid (33% yield); mp 68–70 °C; ^1H NMR (CDCl_3 , 300 MHz), δ (ppm) 8.15 (1H, d, $J = 15.7$ Hz), 8.04 (2H, d, $J = 7.9$ Hz), 7.62 (2H, d, $J = 7.9$ Hz), 7.53 (1H, d, $J = 15.7$ Hz), 7.19 (2H, q, $J = 15.8$ Hz), 7.15 (1H, s), 6.80 (2H, s), 6.54 (1H, s), 5.69 (1H, s), 3.97 (9H, s), 3.92 (6H, s); ^{13}C NMR (75.4 MHz, CDCl_3), δ (ppm) 190.5, 155.1, 152.9, 147.7, 143.7, 141.9, 140.3, 137.8, 135.8, 131.6, 129.4, 128.9, 126.6, 126.2, 120.6, 116.0, 112.0, 104.1, 97.3, 57.0, 56.7, and 56.5. HRMS-ESI: m/z $[\text{M} + \text{H}]^+$ for $\text{C}_{28}\text{H}_{28}\text{O}_7$, calculated 477.1907; observed 477.1902.

(2E)-1-[4-[(E)-2-(4-Hydroxy-3,5-dimethoxyphenyl)ethenyl]phenyl]-3-(2,3,4-trimethoxyphenyl)prop-2-en-1-one (12). Brick red solid (25% yield); mp 100–102 °C; ^1H NMR (CDCl_3 , 300 MHz), δ (ppm) 8.06 (3H, t, $J = 8.5$ Hz), 7.63 (3H, t, $J = 8.5$ Hz), 7.44 (1H, d, $J = 8.7$ Hz), 7.21 (2H, q, $J = 16.2$ Hz), 6.81 (2H, s), 6.76 (1H, d, $J = 7.9$ Hz), 5.68 (1H, s), 3.98 (9H, s), 3.92 (6H, s); ^{13}C NMR (75.4 MHz, CDCl_3), δ (ppm) 190.4, 156.2, 154.2, 147.7, 142.1, 140.3, 137.5, 135.8, 131.8, 129.5, 128.8, 126.6, 126.1, 124.3, 122.5, 121.7, 117.0, 108.0, 104.1, 61.8, 61.3, 56.7, and 56.5. HRMS-ESI: m/z $[\text{M} + \text{H}]^+$ for $\text{C}_{28}\text{H}_{28}\text{O}_7$, calculated 477.1907; observed 477.1919.

(2E)-1-[4-[(E)-2-(4-Hydroxy-3,5-dimethoxyphenyl)ethenyl]phenyl]-3-(2,4,6-trimethoxyphenyl)prop-2-en-1-one (13). Dark yellow solid (32% yield); mp 150–152 °C; ^1H NMR (CDCl_3 , 300 MHz), δ (ppm) 8.32 (1H, d, $J = 15.8$ Hz), 8.05 (2H, d, $J = 8.2$ Hz), 7.95 (1H, d, $J = 15.8$ Hz), 7.61 (2H, d, $J = 8.2$ Hz), 7.28 (1H, s), 7.19 (1H, q, $J = 16.9$ Hz), 6.80 (2H, s), 6.16 (2H, s), 5.67 (1H, s), 3.98 (6H, s), 3.93 (6H, s), 3.88 (3H, s); ^{13}C NMR (75.4 MHz, CDCl_3), δ (ppm) 191.6, 163.5, 162.1, 147.7, 141.5, 138.3, 136.2, 135.7, 131.4, 129.4, 129.0, 126.5, 126.4, 122.4, 107.1, 104.1, 91.0, 56.7, 56.2, and 55.8. HRMS-ESI: m/z $[\text{M} + \text{H}]^+$ for $\text{C}_{28}\text{H}_{28}\text{O}_7$, calculated 477.1907; observed 477.1934.

Representative Procedure for the One Pot Synthesis of (2E)-3-[4-[(E)-2-(4-Hydroxy-3,5-dimethoxyphenyl)ethenyl]phenyl]-1-(2,4,5-trimethoxyphenyl)prop-2-en-1-one (14) via Knoevenagel Condensation–Decarboxylation–Heck Sequence (Scheme 2 and Figure 4). To a solution of 2,4,5-trimethoxyacetophenone (3.2 mmol) in methanol (15 mL) were added 10% aqueous NaOH (6 mmol) and 4-iodo benzaldehyde (3 mmol). The reaction mixture was stirred until complete consumption of starting material. The methanol was vacuum evaporated from the above mixture, and the obtained precipitates were washed with dilute HCl, excess water, dried in air, and finally recrystallized with methanol to obtain pure 1-(2,4,5-trimethoxyphenyl)-3-(4-iodophenyl)prop-2-en-1-one (90% yield).

In the second step, to the stirred mixture of malonic acid (8.4 mmol) and piperidine (10.60 mmol) in DMF (20 mL) were added 4-hydroxy-3,5-dimethoxybenzaldehyde (2.12 mmol), $\text{Pd}(\text{PPh}_3)_4$ (0.035 mmol), LiCl (0.09 mmol), and the reaction mixture was refluxed for 14 h. The above mixture was cooled to room temperature and filtered through Celite. The filtrate was poured into water (100 mL, acidified with dilute HCl, pH 5–6) and extracted with ethyl acetate (2×40 mL). The combined organic layer was washed with water (2×15 mL), brine (1×10 mL), dried over Na_2SO_4 , and vacuum evaporated. The residue was subsequently purified by column chromatography on silica gel (60–120 mesh size) using hexane/ethyl acetate (9:3:0.7) to give product 14.

(2E)-3-[4-[(E)-2-(4-Hydroxy-3,5-dimethoxyphenyl)ethenyl]phenyl]-1-(2,4,5-trimethoxyphenyl)prop-2-en-1-one (14). Orange solid (31% yield); mp 95–97 °C; ^1H NMR (CDCl_3 , 300 MHz), δ (ppm) 7.71 (2H, d, $J = 11.8$ Hz), 7.62 (4H, q, $J = 8.0$ Hz), 7.41 (1H, s), 7.13 (2H, q), 6.78 (2H, s), 6.56 (1H, s), 5.67 (1H, s), 3.98 (3H, s), 3.96 (9H, s), 3.95 (3H, s); ^{13}C NMR (75.4 MHz, CDCl_3), δ (ppm) 190.2, 155.2, 154.0, 147.7, 143.8, 141.9, 139.6, 135.6, 134.9, 130.4, 129.2, 129.1, 127.0, 126.5, 120.9, 113.6, 103.9, 97.6, 57.3,

56.7, and 56.5. HRMS-ESI: m/z $[\text{M} + \text{H}]^+$ for $\text{C}_{28}\text{H}_{28}\text{O}_7$, calculated 477.1907; observed 477.1946.

Synthesis of Other Hydroxylated Stilbene–Chalcone Hybrids Including 15 and 16 (Scheme 2 and Figure 4). The above procedure was followed.

(2E)-3-[4-[(E)-2-(4-Hydroxy-3,5-dimethoxyphenyl)ethenyl]phenyl]-1-(4-methoxyphenyl)prop-2-en-1-one (15). Dark yellow solid (29% yield); mp 189–191 °C; ^1H NMR (CDCl_3 , 300 MHz), δ (ppm) 8.08 (3H, s), 7.80–7.57 (5H, m), 7.01 (4H, s), 6.80 (2H, s), 5.67 (1H, s), 3.97 (9H, s); ^{13}C NMR (75.4 MHz, CDCl_3), δ (ppm) 189.0, 163.8, 147.7, 143.9, 140.0, 135.7, 134.4, 131.6, 131.2, 130.7, 129.3, 129.0, 127.1, 126.4, 121.7, 114.2, 104.0, 56.7, and 55.9. HRMS-ESI: m/z $[\text{M} + \text{H}]^+$ for $\text{C}_{26}\text{H}_{24}\text{O}_5$, calculated 417.1696; observed 417.1659.

(2E)-3-[4-[(E)-2-(4-Hydroxy-3-methoxyphenyl)ethenyl]phenyl]-1-(4-methoxyphenyl)prop-2-en-1-one (16). Brownish yellow solid (28% yield); mp 148–150 °C; ^1H NMR (CDCl_3 , 300 MHz), δ (ppm) 8.08 (2H, s), 7.85 (1H, s), 7.65–7.52 (6H, m), 7.16–6.93 (6H, m), 5.61 (1H, s), 3.97 (3H, s), 3.91 (3H, s); ^{13}C NMR (75.4 MHz, CDCl_3), δ (ppm) 189.1, 163.8, 147.2, 146.4, 143.9, 140.2, 134.3, 131.6, 131.2, 130.5, 130.0, 129.3, 127.1, 126.0, 121.6, 121.2, 115.1, 114.2, 108.8, 56.3, and 53.8. HRMS-ESI: m/z $[\text{M} + \text{H}]^+$ for $\text{C}_{25}\text{H}_{22}\text{O}_4$, calculated 387.1590; observed 387.1561.

Representative Procedure for the Methylation of 11 into (2E)-1-[4-[(E)-2-(3,4,5-Trimethoxyphenyl)ethenyl]phenyl]-3-(2,4,5-trimethoxyphenyl)prop-2-en-1-one (17) (Scheme 3). To a stirred mixture of 11 (0.2 g, mmol) in acetone (8 mL) were added K_2CO_3 (0.84 mmol) and dimethyl sulfate (0.84 mmol). The reaction mixture was refluxed for 24 h. After the usual workup, the residue was purified by column chromatography (hexane/ethyl acetate) to obtain product 17.

(2E)-1-[4-[(E)-2-(3,4,5-Trimethoxyphenyl)ethenyl]phenyl]-3-(2,4,5-trimethoxyphenyl)prop-2-en-1-one (17). Dark orange semi solid (75% yield); ^1H NMR (CDCl_3 , 300 MHz), δ (ppm) 8.13–7.91 (3H, m), 7.56–7.38 (3H, m), 7.11 (2H, t, $J = 14.4$ Hz), 6.76 (2H, s), 6.59–6.46 (2H, m), 3.87 (18H, s); ^{13}C NMR (75.4 MHz, CDCl_3), δ (ppm) 190.2, 154.7, 154.0, 149.7, 143.8, 141.9, 138.4, 137.2, 132.0, 130.4, 129.2, 128.5, 127.1, 126.4, 119.9, 113.6, 105.5, 103.9, 97.6, 60.9, 56.5, 56.3, and 56.1. HRMS-ESI: m/z $[\text{M} + \text{H}]^+$ for $\text{C}_{29}\text{H}_{30}\text{O}_7$, calculated 491.2064; observed 491.2035.

Representative Procedure for the Acetylation of 11 into 2,6-Dimethoxy-4-[(E)-2-[4-[(2E)-3-(2,4,5-trimethoxyphenyl)prop-2-enoyl]phenyl]ethenyl]phenyl Acetate (18) (Scheme 3). To a stirred mixture of 11 (0.2 g, 0.42 mmol) in DMF (8 mL) were added acetic anhydride (1.7 mmol), sodium acetate (1.7 mmol), and a catalytic amount of DMAP (dimethylaminopyridine). The reaction mixture was allowed to stir for 3 h until completion of the reaction. Then the reaction mixture was poured into water (50 mL) and extracted with ethyl acetate (2×20 mL). The combined organic layer was washed with water (2×10 mL), brine (1×10 mL), dried over Na_2SO_4 , and vacuum evaporated. The obtained residue was purified by washing with hexane and ether to give product 18.

2,6-Dimethoxy-4-[(E)-2-[4-[(2E)-3-(2,4,5-trimethoxyphenyl)prop-2-enoyl]phenyl]ethenyl]phenyl Acetate (18). Orange solid (78% yield); mp 170–172 °C; ^1H NMR (CDCl_3 , 300 MHz), δ (ppm) 8.16 (1H, d, $J = 15.7$ Hz), 8.05 (2H, d, $J = 8.1$ Hz), 7.63 (2H, d, $J = 8.1$ Hz), 7.51 (1H, d, $J = 15.7$ Hz), 7.20–7.05 (3H, m), 6.79 (2H, s), 6.53 (1H, s), 3.96 (3H, s), 3.92 (6H, s), 3.89 (6H, s), 2.37 (3H, s); ^{13}C NMR (75.4 MHz, CDCl_3), δ (ppm) 190.5, 169.1, 155.1, 153.0, 152.7, 143.7, 141.4, 140.4, 138.2, 137.2, 135.7, 131.2, 129.4, 129.2, 128.4, 126.9, 115.9, 111.9, 103.8, 97.3, 57.0, 56.8, 56.6, 56.5, and 20.9. HRMS-ESI: m/z $[\text{M} + \text{H}]^+$ for $\text{C}_{30}\text{H}_{30}\text{O}_8$, calculated 519.2013; observed 519.2026.

Representative Procedure for the Sulfonylation of 11 into 2,6-Dimethoxy-4-[(E)-2-[4-[(2E)-3-(2,4,5-trimethoxyphenyl)prop-2-enoyl]phenyl]ethenyl]phenyl-4-methylbenzene-1-sulfonyl (19) (Scheme 3). To a stirred mixture of 11 (0.2 g, 0.42 mmol) in DMF (8 mL) was added pyridine (1.2 mmol) at room temperature followed by *p*-toluenesulfonyl chloride (0.42 mmol) and then a catalytic amount of DMAP (dimethylaminopyridine). The reaction mixture was allowed to stir for 2 h until completion of the

reaction. The reaction mixture was poured into water (50 mL, acidified with dilute HCl, pH 5–6) and extracted with ethyl acetate (2 × 20 mL). The combined organic layer was washed with water (2 × 10 mL), brine (1 × 10 mL), dried over Na₂SO₄, and vacuum evaporated. The obtained residue was subsequently washed with hexane and diethyl ether to obtain the product 19.

2,6-Dimethoxy-4-[(E)-2-[4-[(2E)-3-(2,4,5-trimethoxyphenyl)prop-2-en-1-yl]phenyl]ethenyl]phenyl-4-methylbenzene-1-sulfonate (19). Yellow solid (64% yield); mp 90–92 °C; ¹H NMR (CDCl₃, 300 MHz), δ (ppm) 8.15 (1H, d, J = 15.7 Hz), 8.03 (2H, d, J = 8.0 Hz), 7.88 (2H, d, J = 8.0 Hz), 7.60 (2H, d, J = 8.1 Hz), 7.50 (1H, d, J = 15.7 Hz), 7.35 (2H, d, J = 8.1 Hz), 7.13 (1H, s), 7.09 (2H, d, J = 4.7 Hz), 6.70 (2H, s), 6.51 (1H, s), 3.93 (3H, s), 3.90 (3H, s), 3.89 (3H, s), 3.72 (6H, s), 2.46 (3H, s); ¹³C NMR (75.4 MHz, CDCl₃), δ (ppm) 190.4, 155.1, 153.8, 153.0, 144.9, 143.7, 141.2, 140.4, 138.3, 136.7, 135.3, 130.8, 129.6, 129.4, 129.1, 128.8, 128.4, 127.0, 120.3, 115.9, 111.8, 103.8, 97.2, 57.0, 56.7, 56.5, 56.4, and 20.1. HRMS-ESI: *m/z* [M + H]⁺ for C₃₅H₃₄O₉S, calculated 631.1996; observed 631.1978.

Synthesis of Another Sulfonyl Derivative 20 (Scheme 3).

The same procedure was followed.

2,6-Dimethoxy-4-[(E)-2-[4-[(2E)-3-(2,4,5-trimethoxyphenyl)prop-2-en-1-yl]phenyl]ethenyl]phenyl 3,5-dichlorobenzene-1-sulfonate (20). Yellow solid (63% yield); mp 217–218 °C; ¹H NMR (CDCl₃, 300 MHz), δ (ppm) 8.16 (1H, d, J = 15.7 Hz), 8.11 (2H, d, J = 8.0 Hz), 7.92 (2H, s), 7.66 (3H, t, J = 6.8 Hz), 7.51 (1H, d, J = 15.7 Hz), 7.15 (3H, t, J = 3.5 Hz), 6.75 (2H, s), 6.54 (1H, s), 3.97 (3H, s), 3.93 (6H, s), 3.82 (6H, s); ¹³C NMR (75.4 MHz, CDCl₃), δ (ppm) 190.5, 171.5, 155.2, 153.6, 153.0, 143.7, 141.0, 140.9, 140.5, 138.5, 137.2, 135.9, 133.8, 130.6, 129.5, 128.1, 127.2, 127.0, 120.4, 115.9, 111.9, 103.7, 97.3, 60.7, 57.0, 56.8, and 56.4. HRMS-ESI: *m/z* [M + H]⁺ for C₃₄H₃₀O₉SCl₂, calculated 685.1060; observed 685.1047.

Representative Procedure for the Synthesis of 4-Hydroxy-3,4',5-trimethoxystilbene (21) (Scheme 4). Malonic acid (6.15 mmol) was taken in a round-bottom flask, and piperidine (4.6 mmol) was added gradually. The above mixture was stirred in DMF (15 mL) for 2 min at room temperature. Thereafter, 4-hydroxy-3,5-dimethoxybenzaldehyde (1.51 mmol), *p*-methoxyiodoanisole (0.85 mmol), Pd(PPh₃)₄ (0.025 mmol), piperidine (3.1 mmol), and LiCl (0.07 mmol) were added, and the reaction mixture was allowed to reflux for 14 h. The above mixture was cooled to room temperature and filtered through Celite. The filtrate was poured into water (100 mL, acidified with dilute HCl, pH 5–6) and extracted with ethyl acetate (2 × 40 mL). The combined organic layer was washed with water (1 × 30 mL), brine (1 × 10 mL), dried over Na₂SO₄, and vacuum evaporated. The residue was subsequently purified by column chromatography on silica gel (60–120 mesh size) using hexane/ethyl acetate to give a solid which was further recrystallized in methanol to provide pure product 21.

4-Hydroxy-3,4',5-trimethoxystilbene^{11c} (21). White solid (52% yield); mp 96–98 °C; ¹H NMR (CDCl₃, 300 MHz), δ (ppm) 7.46 (2H, d, J = 6.9 Hz), 6.98–6.90 (4H, m), 6.75 (2H, s), 5.60 (1H, s), 3.96 (6H, s), 3.85 (3H, s); ¹³C NMR (75.4 MHz, CDCl₃), δ (ppm) 159.2, 147.3, 134.6, 130.3, 129.4, 127.5, 126.9, 126.5, 114.2, 103.2, 56.4, and 55.4.

Synthesis of ((E,E)-1,4-Bis(4-hydroxy-3,5-dimethoxy)styryl)benzene (22) (Scheme 4). The same procedure was followed except the equivalents of the respective benzaldehyde, malonic acid, piperidine, Pd catalyst, and LiCl were doubled.

((E,E)-1,4-Bis(4-hydroxy-3,5-dimethoxy)styryl)benzene^{11c} (22). Greenish brown solid (65% yield); mp 246–250 °C; ¹H NMR (DMSO, 300 MHz), δ (ppm) 8.45 (2H, s), 7.46 (4H, s), 7.06 (2H, d, J = 16.4 Hz), 7.05 (2H, d, J = 16.4 Hz), 6.82 (4H, s), 3.74 (12H, s); ¹³C NMR (75.4 MHz, DMSO), δ (ppm) 148.6, 136.8, 136.3, 129.1, 128.1, 125.9, 124.6, 104.7, and 55.7. HRMS-ESI: *m/z* [M + H]⁺ for C₂₆H₂₆O₆, calculated 435.4984; observed 435.4967.

Representative Procedure for the Synthesis of 1-(4-Methoxyphenyl)-3-(2,4,5-trimethoxyphenyl)prop-2-en-1-one (23) (Scheme 5). To a solution of 4-methoxyacetophenone (0.42 g, 3.2 mmol) in methanol (15 mL) were added 10% aqueous NaOH (6 mmol) and 2,4,5-trimethoxybenzaldehyde (0.6 g, 3 mmol). The

reaction mixture was stirred until complete consumption of starting material. Methanol was vacuum evaporated from the above mixture, and the precipitate obtained was washed with dilute HCl, excess water, dried in air, and finally recrystallized with methanol to obtain the pure product 23.

1-(4-Methoxyphenyl)-3-(2,4,5-trimethoxyphenyl)prop-2-en-1-one^{10e} (23). Yellow solid (81% yield); mp 122–124 °C; ¹H NMR (CDCl₃, 300 MHz), δ (ppm) 8.11 (1H, d, J = 15.7 Hz), 8.05 (2H, J = 7.0 Hz), 7.51 (1H, d, J = 15.7 Hz), 7.14 (1H, s), 7.00 (2H, d, J = 9.7 Hz), 6.53 (1H, s), 3.94 (3H, s), 3.91 (6H, s), 3.89 (3H, s); ¹³C NMR (75.4 MHz, CDCl₃), δ (ppm) 189.7, 163.5, 154.9, 152.7, 143.7, 139.7, 132.1, 131.1, 120.6, 116.2, 114.1, 112.1, 97.5, 57.3, 56.8, 56.5, and 55.8.

Synthesis of (2E)-1-{3-[(1E)-3-Oxo-3-(2,4,5-trimethoxyphenyl)prop-1-en-1-yl]phenyl}-3-(2,4,5-trimethoxyphenyl)prop-2-en-1-one (24) (Scheme 5). The above procedure was followed except that the equivalents of the respective benzaldehyde and NaOH were doubled.

(2E)-1-{3-[(1E)-3-Oxo-3-(2,4,5-trimethoxyphenyl)prop-1-en-1-yl]phenyl}-3-(2,4,5-trimethoxyphenyl)prop-2-en-1-one(24). Yellow solid (78% yield); mp 152–154 °C; ¹H NMR (CDCl₃, 300 MHz), δ (ppm) 8.63 (1H, s), 8.22–8.19 (3H, m), 8.14 (1H, s), 7.66 (1H, t, J = 7.7 Hz), 7.55 (2H, d, J = 15.7 Hz), 7.16 (2H, s), 6.54 (2H, s), 3.96 (9H, s), 3.92 (9H, s); ¹³C NMR (75.4 MHz, CDCl₃), δ (ppm) 190.9, 155.3, 153.2, 143.8, 141.3, 139.5, 132.4, 129.2, 128.7, 120.3, 115.7, 111.8, 97.2, 57.0, 56.8, and 56.5. HRMS-ESI: *m/z* [M + H]⁺ for C₃₀H₃₀O₈, calculated 519.2013; observed 519.2051.

Measurement of Inhibition of *P. falciparum* Growth in Culture. In this study chloroquine sensitive Pf3D7 and chloroquine resistant Pf Dd2 and Pf INDO strains were used in vitro culture. Parasite strains were cultivated by the method of Trager and Jensen^{1a} with minor modifications. Cultures were maintained in fresh O+ human erythrocytes at 4% hematocrit in complete medium (RPMI 1640 with 0.2% sodium bicarbonate, 0.5% Albumax, 45 mg/L hypoxanthine, and 50 mg/L gentamicin) at 37 °C under reduced O₂ (gas mixture 5% O₂, 5% CO₂, and 90% N₂). Stock solutions of chloroquine (CQ) were prepared in water (Milli-Q grade), and test compounds were dissolved in DMSO. All stocks were then diluted with complete culture medium to achieve the required concentrations. (In all cases the final concentration was 0.4% DMSO, which was found to be nontoxic to the parasite.) CQ and test compounds were then placed in triplicate wells of 96-well flat-bottom tissue culture grade plates with drug concentrations ranging from 0 to 100 μM in a final well volume of 100 μL for primary screening. Chloroquine was used as a positive control in all experiments. Parasite culture was synchronized at ring stage with 5% sorbitol. Synchronized culture was aliquoted to drug containing 96-well plate at 2% hematocrit and 1% parasitemia. After 48 h of incubation under standard culture conditions, plates were harvested and read by the SYBR Green I fluorescence-based method¹³ using a 96-well fluorescence plate reader (Victor, Perkin-Elmer), with excitation and emission wavelengths of 497 and 520 nm, respectively. The fluorescence readings were plotted against drug concentration, and IC₅₀ values were obtained by visual matching of the drug concentration giving 50% inhibition of growth.

Measurement of Cytotoxic Activity against Mammalian Cell Lines in Culture. Animal cell lines (HeLa and fibroblast L929) were used to determine drug toxicity by using MTT assay for mammalian cell viability assay as described by Mosmann 1983³⁶ using HeLa and fibroblast L929 cells cultured in complete RPMI (cRPMI) containing 10% fetal bovine serum, 0.2% sodium bicarbonate, 50 μg/mL gentamycin. Briefly, cells (10⁴ cells/200 μL/well) were seeded into 96-well flat-bottom tissue-culture plates in complete culture medium. Drug solutions were added after overnight seeding and incubated for 24 h in a humidified atmosphere at 37 °C and 5% CO₂. DMSO (final concentration 10%) was added as +ve control. An aliquot of a stock solution of 3-(4,5-dimethylthiazol-2-yl)-2,5-diphenyltetrazolium bromide (MTT) (5 mg/mL in 1× phosphate-buffered saline) was added at 20 μL per well and incubated for another 3 h. After the plate was spun at 1500 rpm for 5 min, the supernatant was removed and 100 μL of the stop agent DMSO was added to the well to dissolve the formazan crystals. Formation of formazan, an index of growth, was

read at 570 nm by 96-well plate reader (Versa Max), and IC_{50} values were determined by analysis of dose–response curves. The therapeutic index was calculated as $IC_{50}(\text{mammalian cell})/IC_{50}(Pf\ 3D7)$.

Fluorimetric Assay for Falcipain-2 Activity. Recombinant falcipain-2 was purified as described by Shenai et al.³⁷ with minor modifications. The falcipain-2 activity was measured by 96-well plate based high throughput fluorimetric method. Briefly the enzyme (2 μg) was incubated for 10 min at room temperature in 100 mM sodium acetate buffer, pH 5.5, and 10 mM DTT with or without test compounds in triplicate format. The test compound stocks were prepared in DMSO (1% final concentration of DMSO was maintained in all wells). E64 was used as a positive control for falcipain-2. After incubation, substrate benzyloxycarbonyl-Phe-Arg-7-amino-4-methylcoumarin hydrochloride (ZFR-AMC (Sigma), 1 mM stock in DMSO, 2 μL) was added to a final concentration of 10 μM in the same mixture. The enzyme cleaved the substrate and released fluorescent 7-amino-4-methylcoumarin (AMC). The fluorescence was monitored using a 96-well fluorescence plate reader (Victor, Perkin-Elmer), with excitation and emission wavelengths of 355 and 460 nm, respectively. The fluorescence readings were plotted against drug concentration, and IC_{50} values were obtained by visual matching of the drug concentration giving 50% inhibition of enzyme activity.

In Vitro Stage-Specific Inhibition Assay. In order to find if there was stage specificity in the action of the molecules under study, highly synchronized *P. falciparum* (3D7) cultures at ring (R), trophozoite (T), and schizont (S) stages were treated with the two most potent compounds at their respective IC_{100} (11, 6 μM ; 18, 10 μM). The assay was done in two sets of triplicates, one each for the Giemsa stain and SYBR Green assay. Drug pressures were maintained over 48, 24, and 8 h for ring, trophozoite, and schizont stages, respectively, following which the drugs were removed by media wash and the cultures were maintained in drug free complete RPMI medium for 48 h. Percentage of stage-specific inhibition of each compound was calculated in comparison to drug free control by microscopic counting of 3000 cells for each stage and independently assessed for growth by SYBR Green fluorescence assay as described earlier. Parasitized and nonparasitized cells were counted by using Plasmodium auto count 0.1 software developed by Ma et al.³⁸ The parasites with pycnotic morphology were considered as nonviable cells.

Microscopic Evaluation of the Minimal Duration of 11/18–*P. falciparum* Ring/Trophozoite Exposure Necessary for Causing Growth Inhibition. *Plasmodium falciparum* (3D7) ring stage cultures were treated with IC_{100} for 18, 24, and 48 h. Similarly, trophozoite stage cultures were treated with IC_{100} for 18 and 24 h. After the respective incubation periods, drug pressures were removed by media wash and the cultures were maintained under normal culture conditions for a total of 96 h in each case. After this incubation period, thin blood smears were prepared from control and treated wells and processed for Giemsa staining. Percentage of stage-specific inhibition by each compound was calculated in comparison to the corresponding drug free control by counting 3000 cells for each stage as described earlier.

Egress and Invasion Not Affected by 11 and 18. Highly synchronized schizont stage *Plasmodium falciparum* (3D7) cultures were treated with IC_{100} of 11 and 18 and incubated in normal culture conditions for 8 h. The untreated parasites were maintained as control. After incubation, drug pressure was removed by media wash and the washed cultures were incubated for 48 h with or without drug pressure. Thin smears were prepared from control and treated wells and processed for Giemsa staining. The drug effects were monitored microscopically and compared with control.

***P. falciparum* DNA Staining by Hoechst 33342.** Hoechst 33342 (2'-[4-ethoxyphenyl]-5-[4-methyl-1-piperazinyl]-2,5'-bis-1H-benzimidazole trihydrochloride trihydrate, Invitrogen) was used to detect chromatin condensation. DNA minor groove binding Hoechst 33342 is a cell permeable fluorescent dye that emits blue fluorescence at 460 nm. It stains the condensed chromatin of apoptotic cells more brightly than the relaxed chromatin of healthy cells. Briefly, *Plasmodium falciparum* (3D7) ring stage cultures were treated with IC_{100} of test drugs for 24, 42, and 48 h. Similarly, trophozoite stage

cultures were treated with IC_{100} for 18 and 24 h. The treated and untreated parasites were incubated with Hoechst 33342 stain for 10 min at room temperature. Then the parasites were washed with PBS and thin smears were prepared. The slides were observed by using a fluorescence microscope (Nikon 50i).

Determination of *P. falciparum* Mitochondrial Membrane Potential ($\Delta\Psi_m$). *Plasmodium falciparum* mitochondrial membrane potential ($\Delta\Psi_m$) was determined by using JC-1 dye. Cell-permeable cationic carbocyanine dye JC-1 (Invitrogen), also known as 5,5',6,6'-tetrachloro-1,1',3,3'-tetraethylbenzimidazolylcarbocyanine iodine, emits green fluorescence (525 nm) in its monomeric form. However, upon transfer to the membrane environment of a functionally active mitochondrion, it exhibits an aggregation dependent orange-red fluorescence (emission at 590 nm). Briefly, *Plasmodium falciparum* cultures were treated with IC_{100} of test drugs for 24, 42, and 48 h (ring stage culture) or for 18 and 24 h (trophozoite stage cultures). After drug treatment the parasites were incubated with JC-1 dye for 20 min at 37 °C. The wet mounts of stained cultures were observed by using a fluorescence microscope (Nikon 50i).

■ ASSOCIATED CONTENT

📄 Supporting Information

Additional experimental details and NMR (¹H and ¹³C) and HRMS spectra of compounds. This material is available free of charge via the Internet at <http://pubs.acs.org>.

■ AUTHOR INFORMATION

Corresponding Author

*For A.K.S.: phone, 01894-230426; fax, 91-1894-230433; e-mail, aksinha08@rediffmail.com. For D.S.: phone, +91-11-26742357; fax, +91-11-26742316; e-mail, dinkar@icgeb.res.in.

Present Address

[§]Department of Chemistry, Katholieke Universiteit Leuven, Celestijnenlaan 200F, B-3001, Leuven, Belgium.

Author Contributions

^{||}These authors contributed equally.

■ ACKNOWLEDGMENTS

We graciously acknowledge Department of Science and Technology, New Delhi, India (Vide Grant No. SR/S1/OC-16/2008) and the I.H.B.T., Palampur, India (Grant MLP 0025) for financial support. The authors gratefully acknowledge the Directors of I.H.B.T., C.S.I.R., Palampur, and I.C.G.E.B, New Delhi, India, for their kind encouragement as well as providing infrastructure for conducting the above work. N.S. and A.S. are indebted to CSIR, New Delhi, for a Senior Research fellowship. D.M. and D.S. thank MR4 who generously provided the chloroquine resistant Dd2 and INDO strains used in the study. Thanks are extended to David Walliker and X. Su who deposited these strains with MR4. We thank Dr. Pawan Malhotra and Sri Vidya Sundaraman for providing recombinant falcipain-2 and Dr. R. L. Coppel and Charles Ma for Plasmodium auto count 0.1 software. We are thankful to S. Kumar for technical support regarding NMR spectra and HRMS recordings (IHBT Communication No. 2252).

■ ABBREVIATIONS USED

S-C, stilbene–chalcone; DNA, deoxyribonucleic acid; PCD, programmed cell death; SAR, structure–activity relationship; CQ, chloroquine; *Pf*, *Plasmodium falciparum*

■ REFERENCES

(1) (a) Trager, W.; Jensen, J. B. Human malaria parasites in continuous culture. *Science* **1976**, *193*, 673–675. (b) *World Malaria*

Report 2008; World Health Organization: Geneva, Switzerland, 2008. (c) D'hooghe, M.; Dekeukeleire, S.; Mollet, K.; Lategan, C.; Smith, P. J.; Chibale, K.; Kimpe, N. D. Synthesis of novel 2-alkoxy-3-amino-3-arylpropan-1-ols and 5-alkoxy-4-aryl-1,3-oxazinanes with antimalarial activity. *J. Med. Chem.* **2009**, *52*, 4058–4062.

(2) (a) Bjorkman, A. Drug Resistance-Changing Patterns. In *Malaria, Waiting for the Vaccine*; Target, G., Ed.; John Wiley & Sons: Chichester, U.K., 1991; Vol. 27, pp 105–120. (b) Burrows, J. N.; Chibale, K.; Wells, T. N. The state of the art in antimalarial drug discovery and development. *Curr. Top. Med. Chem.* **2011**, *11*, 1226–1254.

(3) (a) Dondorp, A. M.; Nosten, F.; Yi, P.; Das, D.; Phyto, A. P.; Tarning, J.; Lwin, K. M.; Ariey, F.; Hanpithakpong, W.; Lee, S. J.; Ringwald, P.; Silamut, K.; Imwong, M.; Chotivanich, K.; Lim, P.; Herdman, T.; An, S. S.; Yeung, S.; Singhasivanon, P.; Day, N. P. J.; Lindegardh, N.; Socheat, D.; White, N. J. Artemisinin resistance in *Plasmodium falciparum* malaria. *N. Engl. J. Med.* **2009**, *361*, 455–467. (b) Noedl, H.; Se, Y.; Socheat, D.; Fukuda, M. M. Evidence of artemisinin-resistant malaria in Western Cambodia. *N. Engl. J. Med.* **2008**, *359*, 2619–2620. (c) White, N. J. Artemisinin resistance: the clock is ticking. *Lancet* **2010**, *376*, 2051–2052.

(4) (a) WHO Guidelines for the Treatment of Malaria; World Health Organization: Geneva, Switzerland, 2006. (b) Global Report on Antimalarial Drug Efficacy and Drug Resistance: 2000–2010; WHO Press: Geneva, Switzerland, 2010.

(5) (a) Francis, W.; Muregi, A. I. Next-generation antimalarial drugs: hybrid molecules as a new strategy in drug design. *Drug Dev. Res.* **2010**, *71*, 20–32. (b) Meunier, B. Hybrid molecules with a dual mode of action: dream or reality? *Acc. Chem. Res.* **2008**, *41*, 69–77. (c) Walsh, J. J.; Bell, A. Hybrid drugs for malaria. *Curr. Pharm. Des.* **2009**, *15*, 2970–2985.

(6) (a) Guantai, E. M.; Ncokazi, K.; Egan, T. J.; Gut, J.; Rosenthal, P. J.; Bhampidipati, R.; Kopinathan, A.; Smith, P. J.; Chibale, K. Enone and chalcone-chloroquinoline hybrid analogues: in silico guided design, synthesis, antiplasmodial activity, in vitro metabolism, and mechanistic studies. *J. Med. Chem.* **2011**, *54*, 3637–3649. (b) Bellot, F.; Cosledan, F.; Vendier, L.; Brocard, J.; Meunier, B.; Robert, A. Trioxaferroquines as new hybrid antimalarial drugs. *J. Med. Chem.* **2010**, *53*, 4103–4109. (c) Gemma, S.; Campiani, G.; Butini, S.; Joshi, B. P.; Kukreja, G.; Coccone, S. S.; Bernetti, M.; Persico, M.; Nacci, V.; Fiorini, I.; Novellino, E.; Taramelli, D.; Basilico, N.; Parapini, S.; Yardley, V.; Croft, S.; Keller-Maerki, S.; Rottmann, M.; Brun, R.; Coletta, M.; Marini, S.; Guiso, G.; Caccia, S.; Fattorusso, C. Combining 4-aminoquinoline- and clotrimazole-based pharmacophores toward innovative and potent hybrid antimalarials. *J. Med. Chem.* **2009**, *52*, 502–513. (d) Gibbons, P.; Verissimo, E.; Araujo, N. C.; Barton, V.; Nixon, G. L.; Amewu, R. K.; Chadwick, J.; Stocks, P. A.; Biagini, G. A.; Srivastava, A.; Rosenthal, P. J.; Gut, J.; Guedes, R. C.; Moreira, R.; Sharma, R.; Berry, N.; Cristiano, M. L. S.; Shone, A. E.; Ward, S. A.; O'Neill, P. M. Endoperoxide carbonyl falcipain 2/3 inhibitor hybrids: toward combination chemotherapy of malaria through a single chemical entity. *J. Med. Chem.* **2010**, *53*, 8202–8206.

(7) (a) Cosledan, F.; Fraisse, L.; Pellet, A.; Guillou, F.; Mordmuller, B.; Kremsner, P. G.; Moreno, A.; Mazier, D.; Maffrand, J. P.; Meunier, B. Selection of a trioxaquine as an antimalarial drug candidate. *Proc. Natl. Acad. Sci. U.S.A.* **2008**, *105*, 17579–17584. (b) Domarle, O.; Blampain, G.; Agnani, H.; Nzadiyabi, T.; Lebibi, J.; Brocard, J.; Maciejewski, L.; Biot, C.; Georges, A. J.; Millet, P. In vitro antimalarial activity of a new organometallic analog, ferrocene-chloroquine. *Antimicrob. Agents Chemother.* **1998**, *42*, 540–544.

(8) Wells, T. N. C.; Alonso, P. L.; Gutteridge, W. E. New medicines to improve control and contribute to the eradication of malaria. *Nat. Rev. Drug Discovery* **2009**, *8*, 879–891.

(9) (a) Jang, M.; Cai, L.; Udeani, G. O.; Slowing, K. V.; Thomas, C. F.; Beecher, C. W. W.; Fong, H. H. S.; Farnsworth, N. R.; Kinghorn, A. D.; Mehta, R. G.; Moon, R. C.; Pezzuto, J. M. Cancer chemopreventive activity of resveratrol, a natural product derived from grapes. *Science* **1997**, *275*, 218–220. (b) Dark, G. G.; Hill, S. A.;

Prise, V. E.; Tozer, G. M.; Pettit, G. R.; Chaplin, D. J. Combretastatin A-4, an agent that displays potent and selective toxicity toward tumor vasculature. *Cancer Res.* **1997**, *57*, 1829–1834. (c) Baur, J. A.; Sinclair, D. A. Therapeutic potential of resveratrol: the in vivo evidence. *Nat. Rev. Drug Discovery* **2006**, *5*, 493–506.

(10) (a) Mankil, J.; Wonhwan, P.; Jaechul, J.; Young, L. E.; Yongnam, L.; Seikwan, O.; Hyung, M. Synthesis, structural characterization and biological evaluation of novel stilbene derivatives as potential antimalarial agents. *Chem. Biol. Drug Des.* **2009**, *73*, 346–354. (b) Choosak, B.; Worrapiroj, O.; Palangpon, K.; Prasat, K.; Morakot, T.; Yodhathai, T. An antimalarial stilbene from *Artocarpus integerifolius*. *Phytochemistry* **2000**, *54*, 415–417. (c) Park, W. H.; Lee, S. J.; Moon, H. I. Antimalarial activity of a new stilbene glycoside from *Parthenocissus tricuspidata* in mice. *Antimicrob. Agents Chemother.* **2008**, *52*, 3451–3453. (d) Li, R.; Chen, X.; Gong, B.; Dominguez, J. N.; Davidson, E.; Kurzban, G.; Miller, R. E.; Nuzum, E. O.; Rosenthal, P. J. In vitro antimalarial activity of chalcones and their derivatives. *J. Med. Chem.* **1995**, *38*, 5031–5037. (e) Kumar, R.; Mohanakrishnan, D.; Sharma, A.; Kaushik, N. K.; Kalia, K.; Sinha, A. K.; Sahal, D. Reinvestigation of structure–activity relationship of methoxylated chalcones as antimalarials: synthesis and evaluation of 2,4,5-trimethoxy substituted patterns as lead candidates derived from abundantly available natural β -asarone. *Eur. J. Med. Chem.* **2010**, *45*, 5292–5301. (f) Sharma, A.; Sharma, N.; Shard, A.; Kumar, R.; Saima; Mohanakrishnan, D.; Sinha, A. K.; Sahal, D. Tandem allylic oxidation–condensation/esterification catalyzed by silica gel: an expeditious approach towards antimalarial diaryldienones and enones from natural methoxylated phenylpropenes. *Org. Biomol. Chem.* **2011**, *9*, 5211–5219.

(11) (a) Sinha, A. K.; Sharma, A.; Joshi, B. P. One-pot two-step synthesis of 4-vinylphenols from 4-hydroxy substituted benzaldehydes under microwave irradiation: a new perspective on the classical Knoevenagel–Doebner reaction. *Tetrahedron* **2007**, *63*, 960–965. (b) Sinha, A. K.; Joshi, B. P.; Sharma, A. Microwave Induced Process for the Preparation of Substituted 4-Vinylphenols. U.S. Patent 6989467, 2006. (c) Sharma, A.; Sharma, N.; Kumar, R.; Shard, A.; Sinha, A. K. Direct olefination of benzaldehydes into hydroxy functionalized oligo (*p*-phenylenevinylene)s via Pd-catalyzed heterodominant Knoevenagel–decarboxylation–Heck sequence and its application for fluoride sensing π -conjugated units. *Chem. Commun.* **2010**, *46*, 3283–3285. (d) Sharma, N.; Sharma, A.; Shard, A.; Kumar, R.; Saima; Sinha, A. K. Pd-catalyzed orthogonal Knoevenagel/Perkin condensation–decarboxylation–Heck/Suzuki sequences: tandem transformations of benzaldehydes into hydroxy-functionalized anti-diabetic stilbene–cinnamoyl hybrids and asymmetric distyrylbenzenes. *Chem.—Eur. J.* **2011**, *17*, 10350–10356. (e) Sinha, A. K.; Kumar, R.; Sharma, A.; Sharma, N. One Pot Multicomponent Synthesis of Some Novel Hydroxy Stilbene Derivatives with alpha, beta-Carbonyl Conjugation under Microwave Irradiation WO/2010/113005, 2010.

(12) (a) Lambert, J. D.; Sang, S.; Hong, J.; Kwon, S. J.; Lee, M. J.; Ho, C. T.; Yang, C. S. Peracetylation as a means of enhancing in vitro bioactivity and bioavailability of epigallocatechin-3-gallate. *Drug Metab. Dispos.* **2006**, *34*, 2111–2116. (b) Kopka, I. E.; Young, D. N.; Lin, L. S.; Mumford, R. A.; Magriotis, P. A.; MacCoss, M.; Mills, S. G.; Ripper, G. V.; McCauley, E.; Egger, L. E.; Kidambi, U.; Schmidt, J. A.; Lyons, K.; Stearns, R.; Vincent, S.; Colletti, A.; Wang, Z.; Tong, S.; Wang, J.; Zheng, S.; Owens, K.; Levorse, D.; Hagemann, W. K. Substituted *N*-(3,5-dichlorobenzenesulfonyl)-*L*-prolyl-phenylalanine analogues as potent VLA-4 antagonists. *Bioorg. Med. Chem. Lett.* **2002**, *12*, 637–640. (c) Golebiowski, A.; Klopfenstein, S. R.; Portlock, D. E. Lead compounds discovered from libraries: part 2. *Curr. Opin. Chem. Biol.* **2003**, *7*, 308–325.

(13) Smilkstein, M.; Sriwilajaro, N.; Kelly, J. X.; Wilairat, P.; Riscoe, M. Simple and inexpensive fluorescence-based technique for high-throughput antimalarial drug screening. *Antimicrob. Agents Chemother.* **2004**, *48*, 1803–1806.

(14) (a) Larrosa, M.; Fransisco, A.; Tomma, S.; Barberra, N.; Espian, J. C. Resveratrol and its analogous 4-hydroxystilbene induce

- growth inhibition, apoptosis, S-phase arrest and upregulation of cyclins A, E and B1 in human SK-Mel-28 melanoma cells. *J. Agric. Food Chem.* **2003**, *51*, 4576–4584. (b) Simoni, D.; Roberti, M.; Invidiata, F. P.; Aiello, E.; Aiello, S.; Marchetti, P.; Baruchello, R.; Eleopra, M.; Cristina, A. D.; Grimaudo, S.; Gebbia, N.; Crosta, L.; Dielig, F.; Tolomeo, M. Stilbene-based anticancer agents: resveratrol analogues active toward HL60 leukemic cells with a non-specific phase mechanism. *Bioorg. Med. Chem. Lett.* **2006**, *16*, 3245–3248.
- (15) Bhattacharya, A.; Mishra, L. C.; Sharma, M.; Awasthi, S. K.; Bhasin, V. K. Antimalarial pharmacodynamics of chalcone derivatives in combination with artemisinin against *Plasmodium falciparum* in vitro. *Eur. J. Med. Chem.* **2009**, *44*, 3388–3393.
- (16) Li, R.; Kenyon, G. L.; Cohen, F. E.; Chen, X.; Gong, B.; Dominguez, J. N.; Davidson, E.; Kurzban, G.; Miller, R. E.; Nuzum, E. O. In vitro antimalarial activity of chalcones and their derivatives. *J. Med. Chem.* **1995**, *38*, 5031–5037.
- (17) Sriwilajaroen, N.; Liu, M.; Go, M. L.; Wilairat, P. Plasmepsin II inhibitory activity of alkoxyated and hydroxylated chalcones. *Southeast Asian J. Trop. Med. Public Health* **2006**, *37*, 607–612.
- (18) Geyer, J. A.; Keenan, S. M.; Woodard, C. L.; Thompson, P. A.; Gerena, L.; Nichols, D. A.; Gutteridge, C. E.; Waters, N. C. Selective inhibition of Pfmrk, a *Plasmodium falciparum* CDK, by antimalarial 1,3-diaryl-2-propenones. *Bioorg. Med. Chem. Lett.* **2009**, *19*, 1982–1985.
- (19) Rosenthal, P. J. Proteases and Hemoglobin Degradation. In *Molecular Approaches to Malaria*; Sherman, I. W., Ed.; ASM Press: Washington, DC, 2005; pp 311–326.
- (20) Dominguez, J. N.; Charris, J. E.; Lobo, G.; Gamboa de Dominguez, N.; Moreno, M. M.; Riggione, F.; Sanchez, E.; Olson, J.; Rosenthal, P. J. Synthesis of quinoliny chalcones and evaluation of their antimalarial activity. *Eur. J. Med. Chem.* **2001**, *36*, 555–560.
- (21) Kerr, J. F. History of the events leading to the formulation of the apoptosis concept. *Toxicology* **2002**, *181–182*, 471–474.
- (22) Gougeon, M. L.; Lecoœur, H. Evaluation of apoptosis. *J. Immunol. Methods* **2002**, *265*, 1–2.
- (23) Debrabant, A.; Lee, N.; Bertholet, S.; Duncan, R.; Nakhasi, H. L. Programmed cell death in trypanosomatids and other unicellular organisms. *Int. J. Parasitol.* **2003**, *33*, 257–267.
- (24) Deponte, M.; Becker, K. *Plasmodium falciparum*—Do killers commit suicide? *Trends Parasitol.* **2004**, *20*, 165–169.
- (25) Picot, S.; Burnod, J.; Bracchi, V.; Chumpitazi, B. F.; Ambroise-Thomas, P. Apoptosis related to chloroquine sensitivity of the human malaria parasite *Plasmodium falciparum*. *Trans. R. Soc. Trop. Med. Hyg.* **1997**, *91*, 590–591.
- (26) Ch'ng, J. H.; Kotturi, S. R.; Chong, A. G.; Lear, M. J.; Tan, K. S. A programmed cell death pathway in the malaria parasite *Plasmodium falciparum* has general features of mammalian apoptosis but is mediated by clan CA cysteine proteases. *Cell Death Dis.* **2010**, *1*, e26.
- (27) Mutai, B. K.; Waitumbi, J. N. Apoptosis stalks *Plasmodium falciparum* maintained in continuous culture condition. *Malar. J.* **2010**, *9* (Suppl.3), S6.
- (28) Meslin, B.; Barnadas, C.; Boni, V.; Latour, C.; De Monbrison, F.; Kaiser, K.; Picot, S. Features of apoptosis in *Plasmodium falciparum* erythrocytic stage through a putative role of PfMCA1 metacaspase-like protein. *J. Infect. Dis.* **2007**, *195*, 1852–1859.
- (29) Lopez, M. L.; Vommaro, R.; Zalis, M.; de Souza, W.; Blair, S.; Segura, C. Induction of cell death on *Plasmodium falciparum* asexual blood stages by *Solanum nudum* steroids. *Parasitol. Int.* **2010**, *59*, 217–225.
- (30) Nyakeriga, A. M.; Perlmann, H.; Hagstedt, M.; Berzins, K.; Troye-Blomberg, M.; Zhivotovsky, B.; Perlmann, P.; Grandien, A. Drug-induced death of the asexual blood stages of *Plasmodium falciparum* occurs without typical signs of apoptosis. *Microbes. Infect.* **2006**, *8*, 1560–1568.
- (31) Totino, P. R.; Daniel-Ribeiro, C. T.; Corte-Real, S.; de Fatima Ferreira-da-Cruz, M. *Plasmodium falciparum*: erythrocytic stages die by autophagic-like cell death under drug pressure. *Exp. Parasitol.* **2008**, *118*, 478–486.
- (32) Al-Olayan, E. M.; Williams, G. T.; Hurd, H. Apoptosis in the malaria protozoan, *Plasmodium berghei*: a possible mechanism for limiting intensity of infection in the mosquito. *Int. J. Parasitol.* **2002**, *32*, 1133–1143.
- (33) Arambage, S. C.; Grant, K. M.; Pardo, I.; Ranford-Cartwright, L.; Hurd, H. Malaria ookinetes exhibit multiple markers for apoptosis-like programmed cell death in vitro. *Parasites Vectors* **2009**, *2*, 32.
- (34) Wyllie, A. H.; Kerr, J. F.; Currie, A. R. Cell death: the significance of apoptosis. *Int. Rev. Cytol.* **1980**, *68*, 251–306.
- (35) Pollitt, L. C.; Colegrave, N.; Khan, S. M.; Sajid, M.; Reece, S. E. Investigating the evolution of apoptosis in malaria parasites: the importance of ecology. *Parasites Vectors* **2010**, *3*, 105.
- (36) Mosmann, T. Rapid colorimetric assay for cellular growth and survival: application to proliferation and cytotoxicity assays. *J. Immunol. Methods* **1983**, *65*, 55–63.
- (37) Shenai, B. R.; Sijwali, P. S.; Singh, A.; Rosenthal, P. J. Characterization of native and recombinant falcipain-2, a principal trophozoite cysteine protease and essential hemoglobinase of *Plasmodium falciparum*. *J. Biol. Chem.* **2000**, *275*, 29000–29010.
- (38) Ma, C.; Harrison, P.; Wang, L.; Coppel, R. L. Automated estimation of parasitaemia of *Plasmodium yoelii*-infected mice by digital image analysis of Giemsa-stained thin blood smears. *Malar. J.* **2010**, *9*, 348.